FABRICATION AND CHARACTERIZATION OF ANTIBACTERIAL POLYCAPROLACTONE AND NATURAL HYDROXYAPATITE NANOFIBERS FOR BONE TISSUE SCAFFOLDS

A Thesis by

Stephanie Marie Patrick

Bachelor of Science, Wichita State University, 2008

Submitted to the Department of Mechanical Engineering
and the faculty of the Graduate School of
Wichita State University
in partial fulfillment of
the requirements for the degree of
Master of Science

May 2013

FABRICATION AND CHARACTERIZATION OF ANTIBACTERIAL POLYCAPROLACTONE AND NATURAL HYDROXYAPATITE NANOFIBERS FOR BONE TISSUE SCAFFOLDS

The following faculty members have examined the final copy of this thesis for form and content, and recommend that it is accepted in partial fulfillment of the requirement for the degree of Master of Science with a major in Mechanical Engineering.

_____
Ramazan Asmatulu, Committee Chair

_____
Hamid Lankarani, Committee Member

_____
Shang-You Yang, Committee Member

DEDICATION

To my husband, my family and friends who have supported me throughout my education

ABSTRACT

Chronic osteomyelitis is a bone infection that may result in pain, pus, bone resorption and damage, and fractures. The disease often needs prolonged antibiotic therapy, and in many cases severe wounds and bone voids are caused by surgical interventions. Autograft, allograft, xenograft, or synthetic materials have been used as bone fillers or scaffolds. Gentamicin is a common antibiotic in osteomyelitis treatment; including gentamicin in the scaffold therefore would help treat the osteomyelitis once the scaffold is in place and help prevent spreading of the disease. Hydroxyapatite (HA) is a mineral that is naturally found in bone that has osteoconductive properties in bone tissue engineering. I hypothesize that a bone graft substitute incorporating both gentamicin and HA would be very beneficial for the treatment of osteomyelitis with large bone damage. While there are many methods to fabricate porous graft using a biodegradable polymer, electrospinning technique is particularly ideal due to nano-fibrous structure resembling the extracellular matrix of bone. The objectives of my thesis work are to develop a gentamicin-contained PCL-HA composite scaffold and to evaluate its therapeutic efficacy in inhibiting E. coli growth using at *in vitro* settings. PCL-HA composite nanofibers were fabricated using electrospinning with inclusions of gentamicin to give the nanofibers antibacterial properties. HA was obtained from cow bone, with SEM and EDS examinations confirming that its chemical structure and size were well suited to promote bone growth. SEM micrographs illustrated the nano-scaled fiber structures with an average diameter of 142.2 nm, and biological tests revealed that the gentamicin-containing PCL-HA nano-fiber membranes effectively exterminated E. coli's growth up to 7 days, with zones of inhibition to 4 cm^2. Further study is warranted to characterize the antibiotic release patterns in vivo and the potential safety issues.

TABLE OF CONTENTS

LIST OF FIGURES

LIST OF FIGURES (continued)

LIST OF FIGURES (continued)

Figure Page

CHAPTER 1

INTRODUCTION

1.1 Background

Osteomyelitis is the inflammation of bone caused by bacterial or fungal infections. These infections can occur after open fractures of the bone or due to infections from implants in hip or knee replacements. [1] [2] Typical treatment of osteomyelitis involves the removal of dead bone tissue as well as up to 4-6 weeks of treatment of the infection with intravenous antibiotics. The void left in the remaining bone from where the dead bone tissue was removed is typically filled with a bone graft. In particular with cases of chronic osteomyelitis, drug delivery systems have been used to directly administer antibiotic to the infected area. [1] [2] [3] Previously, beads of polymer (typically poly (methyl methacrylate) (PMMA)) have been used as a carrier for antibiotics that can be implanted directly into the infected area of bone. [3] While drug delivery was successfully performed using PMMA, its nonbiodegradable property required additional surgery to remove the beads once all of the antibiotics were released. [1] [2] As such, biodegradable beads made out of polymers like poly (D, L-lactide) (PDLLA) with antibiotics have been studied as an alternative to using PMMA. [1] Once the infection is treated, a void can still remain if dead bone tissue was removed that would need to be filled with a graft or allowed to regenerate on its own.

A material that has the ability to release antibiotics, and can be used as a biodegradable graft material would be the most beneficial in this case. In order to ensure sufficient healing of the bone, the material would need to be osteoconductive and support the growth of new bone tissue. Calcium phosphate ceramics like hydroxyapatite (HA) have been shown to provide osteoconductivity both by itself and when incorporated with other materials. [4] [5] [6] [7]

While synthetic versions of HA have been more often used, it can also be derived naturally from sources like cow bone. Incorporating both an antibiotic and HA into a biodegradable polymer like polycaprolactone (PCL) can be a sufficient solution to both treat the infection of osteomyelitis and encourage the growth of new healthy bone tissue.

1.2 Goals

The goal of this project is to create a porous nanofiber structure out of polycaprolactone via electrospinning. Polycaprolactone is a biodegradable polymer that has been used previously for drug delivery as well as scaffold material for bone tissue. Electrospinning is an efficient method of producing nanofibers as well as research has shown that these fibers resemble the natural extracellular matrix of bone. [8] [9] This structure should be antibacterial with the inclusion of gentamicin, able to help with the growth of osteoblast cells with the inclusion of hydroxyapatite, and biocompatible. The HA used will be naturally derived from cow bone and SEM and EDS testing will be done to determine its chemical structure. Testing of the structure's antibacterial properties will be performed with E. coli to determine the success of the inclusion of gentamicin.

CHAPTER 2

LITERATURE REVIEW

2.1 Fundamentals of Bone Structure and Tissue Engineering

2.1.1 Cells, Tissue, and the Skeletal System

The human body has 208 bones all of which are made of three different components: living cells, non-living organic materials, and inorganic crystals. The living cells in the bones are osteoblasts, osteoclasts, and osteocytes. Osteoblasts are the cells that produce new bone. Osteoclasts are cells that reabsorb bone tissue. [10] Osteocytes are the mature bone cells that are no longer growing and not being reabsorbed. [4] Osteocytes can become osteoblasts or osteoclasts again as needed. Collagen is the non-living organic material in bone and is a tough

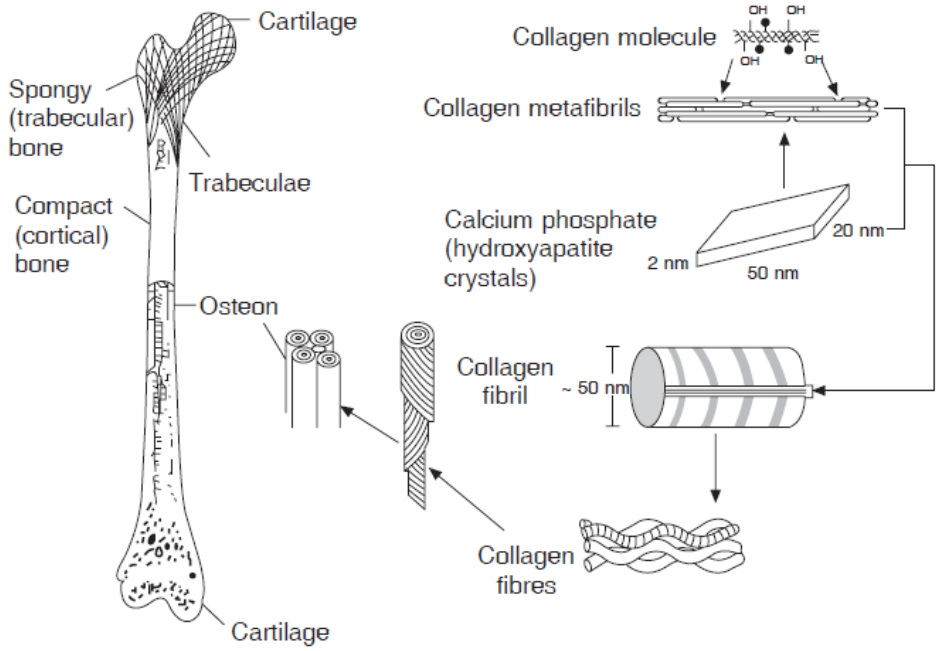

Figure 1: Bone Structure of a femur. **[11]**

protein that is found throughout the body. Hydroxycarbonate apatite (HCA) is a carbonated form of hydroxyapatite (HA) which will be discussed in greater detail later. There are several types of bone structures with the possibility of multiple structures being represented in a single

bone. Figure 1 shows the structure for a femur and in particular the detailed structure of cortical bone. Cortical bone is the strongest of all the different structures of bone. This is due to the dense structure of osteons (running parallel along the length of the bone) within the cortical bone. Osteons are the structure of the collagen fibrils and the apatite crystals that is shown in Figure 1. The second strongest structure of bone is the trabecular bone (also known as cancellous bone or spongy bone). Trabecular bone is much less dense than cortical bone and therefore has a lower strength. The mechanical properties of the cortical bone, trabecular bone, cartilage and tendon are shown in Table 1. Cortical bone is an anisotropic material; its properties depend on whether the bone is subjected to tensile, compressive, or torsional forces. Reference Table 1 for specific mechanical properties. [11]

Table 1: Mechanical properties of select bone tissues. **[12]**

Property	Cortical bone	Cancellous bone	Articular cartilage	Tendon
Compressive strength (MPa)	100–230	2–12		
Flexural, tensile strength	50–150	10–20	10–40	80–120
Strain to failure	1–3	5–7		10
Young's (tensile) modulus	7–30	0.5–0.05		1
Fracture toughness (K_{1c})	2–12			
Compressive stiffness (N)			20–60	
Compressive creep modulus			4–15	
Tensile stiffness (MPa)			50–225	

2.1.2 Inflammation & Wound Healing

The goals for treating bone fractures are to have rapid healing of the bone, restore its function, avoid visually unnatural healing, and to generally avoid any complications such as infections. For bone fractures, depending on the type of fracture, treatments can be surgical or non-surgical. For surgical treatments, external or internal fracture treatments can occur. Examples of non-surgical treatments are casts or braces that immobilize the bone to allow it to heal. Immobilization of the bone is important for bone healing because large movement between

fracture bone segments can cause further injury or delay healing. On the contrary, small movements can enhance healing of a bone fracture. An example of a surgical external fracture treatment is pins that hold the bone segments in alignment that have their ends outside the skin of the body. The pins are then held in place by bars or plates that are also external to the body. Internal surgical fracture treatments include pins, wires, and plates that are completely within the body. Metal materials that are used for internal fracture treatments shouldn't corrode and therefore stay within the body after the fracture has healed. This would require further surgery to remove the materials if discomfort or other complications occur due to the material's presence after fracture healing. [12]

Bone is very adaptable and can regenerate and remodel itself due to a balance between osteogenesis and osteolysis. Osteogenesis refers to the forming of new bone due to osteoblasts; osteolysis refers to the removing of bone due to osteoclasts. The balance between the osteoblast and osteoclast cell activity varies due to dynamic and static stresses on the bone. Figure 2 shows the general process of a bone fracture repair. [12] After initial fracture, inflammation occurs and due to the trauma of an injury that would cause bone fracture, a hematoma is formed from the ruptured blood vessels around the fracture. Bone necrosis can be seen around the ends of the fracture. Osteoclasts remove the dead bone tissue as a soft callus grows around the fractured area. Osteoblasts and fibroblasts are produced to regrow the fractured bone from the end of the fracture. The soft callus connects the fractured pieces of bone during the remainder of the healing process. A hard callus replaces the soft callus a few weeks after the initial injury as minerals like HA are released to form a solid connection over the fracture site. Finally, the original morphology of the bone is achieved during final remodeling of the bone once the fractured area has been completely united. Excess hard callus is eventually removed until the

original shape of bone is achieved. [13] The dark lines in Figure 2 represent osteoblast cells that grow the new bone. [12]

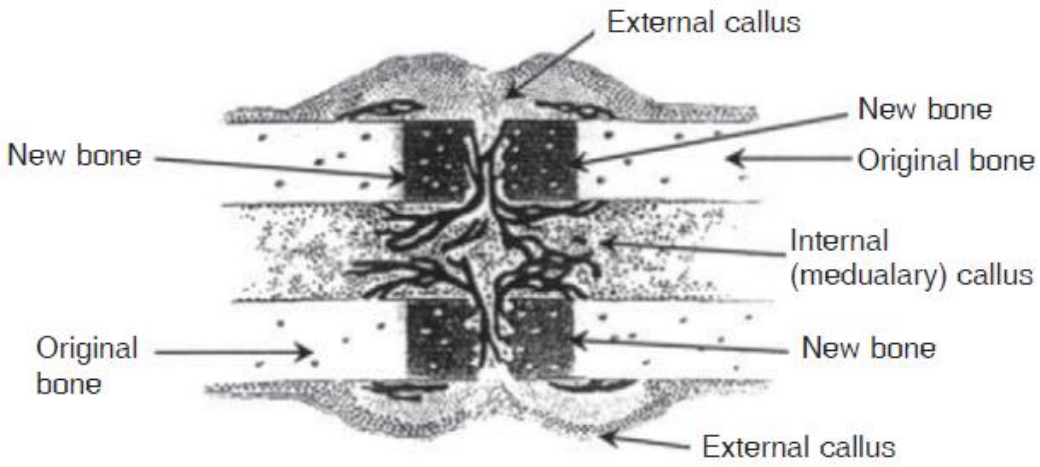

Figure 2: Schematic of the repair of a fracture of a long bone. **[12]**

Implants have an effect on how wounds heal. Most of the effect that implants have on the healing process occurs during step one of the normal wound healing behaviors discussed earlier. Examples of issues with implants that can increase step one of the normal wound healing process include implant movement, implant degradation, toxic leachables from implants, and rough implant surfaces. New blood vessels that would form during healing cannot invade a solid surface that some implants have (they can only run along it), but can invade porous implants. New blood vessels, when allowed to form naturally, help improve healing time. Implants affect step two of normal wound healing because fibroblasts will not produce fibers until larger phagocytes (like macrophages) leave the wounded area, and implants may fill voids where bone tissue is missing. Finally during step three of normal wound healing, the new collagen is aligned along lines of stress which are directly affected by the properties and size of the implant. [14]

As mentioned earlier, wires, pins, screws, and plates can be used to internally immobilize the fracture for repair. Wires are typically used to reattach large pieces of bone or to provide

additional stability to fractures that have been fixed by other means. Pins are basically straight wires that are used to hold pieces of bone together or to guide screws. Screws are the most commonly used device and have two varieties, cortical and cancellous, which correspond with the type of bone they are used for. Plates may be used to add additional structure to a fracture site. Based on the shape and flexibility, plates can have different effects on healing. Plates are held to the bone using screws. Stiff plates help shield the bone from physical loads, while flexible plates allow small motions and physical loads to be applied to the healing bone. Straight plates that are close to the bone can prevent blood vessels from providing nutrients to the outer layers, while plates that are sufficiently separated from the bone can. The shape and stiffness of the plate depends on the type of fracture and type of bone that needs repair. [12]

There is no material that can be implanted that is completely inert; it has some affect on the tissue it is implanted with. As such, a material can be classified as one or more of the following: toxic, nearly inert, bioactive or biodegradable. Toxic materials are ones that kill cells and surrounding tissue either by the material itself or through a leachable chemical in the material. Toxic materials should never be used for implants. Nearly inert materials don't have much of an effect on the cells and tissues once in the body except that a fibrous capsule will form around it during healing. It is known that the thinner the fibrous capsule is around the implant, the more successful the material is as an implant. The capsule is like a protective barrier between the implant and the cells and tissue. Bioactive materials have an interfacial bond between the implant and the surrounding tissue, which gives a specific biological response. A very thin, if any, capsule surrounds the implant. Finally, biodegradable materials are ones that are able to dissolve and be replaced by the surrounding tissue. For implants, it is necessary that the biodegradable materials be non-toxic once dissolved, be able to be easily metabolized out of

the area, and that the replacement rate of new tissue be similar to the rate of implant dissolution. [14]

Large defects or areas of missing bone, such as bone removed during the removal of a tumor, need bone grafts. An autograft of the patient's own bone is the most desired, but is not always possible due to insufficient supply of quality bone. A bone substitute, or allograft, is therefore necessary. Using bioactive materials, the interfacial bond between the graft and the bone would allow for healing of the bone. The bond is created by a layer of HCA that forms on the bioactive materials. This HCA is identical in structure and chemical composition to the crystals mentioned earlier that form osteons in bone. Bioactive materials such as Bioglass® have successfully been used in the repair of small bones and low stress inducing areas of the body on their own. It is possible, though to make a composite of a bioactive material with less brittle materials such as biodegradable polymers that would be able to be used as bone grafts for larger and higher physically stressed bones. [12]

2.1.3 Biological Cell Culturing and Immunochemical Methods

Cells, such as osteoblasts for bone tissue, can be obtained for cell culturing from solid tissues. Cells obtained from solid tissue need a substrate to grow on. Figure 3 shows different types of cells that are grown on a substrate. These cells have different morphologies depending on the tissue the cells came from. The cells divide and multiply once they are attached to the substrate. When they form a complete layer, most types of cells stop growing, so it is ideal to seed these cells when they are about 70-80% to a full layer. In order for cells to survive in vitro, they need the nutrients that are normally provided in vivo, such as carbohydrates, salts, amino acids, vitamins, fatty acids, and proteins. The basal medium that is typically used to culture cells contains nearly all of these nutrients. Fetal bovine serum, which has more proteins, is also

sometimes used. Finally, when seeding cells onto a material it is necessary to know the number of cells/cm^2 to ensure reproducible results. [15]

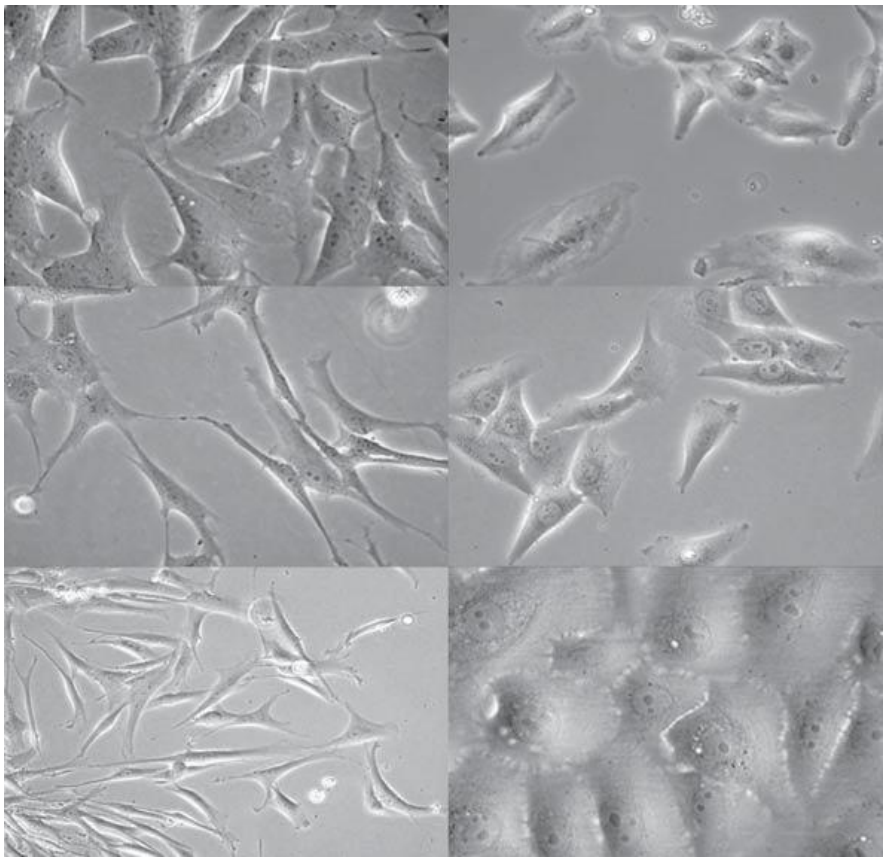

Figure 3: Phase contrast images showing cell morphology of different human cells. Middle left image is of human fetal osteoblasts. **[15]**

While implants were originally designed to be biologically inert, recent research focus on implants, in particular with tissue engineering, has been focusing on biodegradable and bioactive materials due to their abilities to influence the physical environment they are placed in. How the biological area responds to an implant (both in vivo and in vitro) is greatly researched and can be affected by factors including the topography of the implant, its chemical composition, its rate of dissolution (if biodegradable), and its mechanical properties. Implants are designed to encourage specific biological responses once in place. Stents are designed to prevent cells and proteins from adhering to the surface, in order to prevent blood clots. On the other hand, orthopaedic

implants are designed to encourage cell adhesion to the surface so that the implant doesn't loosen. Assurance of successful interaction between the host tissue and the implant is the goal of biological testing. [16]

2.1.4 Clinical Applications and Challenges

While tissue engineering is a great option in the future for growing parts of, or whole, tissue (in particular in cases with organ donor shortages), there are currently still issues that do not make it a completely viable option yet. Some of these issues are the source of seed cells, stable 3-D structures, vascularisation, interfacial stability, sterilization, cost, and survivability. For the source of cells, the issues stem from one of three problems. Cells from the patient provide for the most reliable tissue engineering, but there are usually limitations on the number of cells available. Cloned cells are not good at differentiation, meaning that they cannot produce the many different types of cells necessary for successful tissue engineering. Finally, stem cells have a stigma associated with them, causing them to occasionally be morally or legally unavailable.

Since all tissues have a 3-D structure, a 3-D scaffold is necessary to grow full tissues. Currently most tissue engineering involves growing one or two types of cells on a 2D surface. All tissues need an interconnected blood supply once implanted into the body. Most, when grown outside the body, do not have that vascular system in place for implantation. The body then has to quickly create a blood supply to the new tissue or the cells die. [17] [4] The tissue engineered implants (in particular with bone grafts) need a good interface between the host tissue and the implant. Problems like breakdown of the implant or shrinkage of the implant may also cause undesirable results. Furthermore, it is difficult to keep the engineered tissue sterile and safe for the host tissues, in particular if the tissue is grown in vitro. Many ways of sterilizing

non-living materials would kill the cells that are trying to be grown. The associated costs are an issue, but as technology and research grows, the cost to produce engineered tissue should decrease. Finally, long-term survivability of engineered tissue is still unknown. Obviously, to make cost, surgery and other factors worthwhile to the patient, the new tissue needs to have a long survivability. [18]

Some of the current challenges, in particular with bone tissue engineering, include poor mechanical properties of current scaffolds. The scaffolds also do not completely resemble the physiological properties of the bone it is trying to replace. The cell-extracellular matrix (ECM), or the adhesion of the scaffold to the host tissue do not quite match the structural characteristics that are found in the host tissue. [17] [4] [18]

2.2 Bone Tissue Scaffold Principles

Cells can grow in any cell friendly environment. The purpose of scaffolds for tissue engineering, and bone tissue engineering in particular, is to let cells grow and proliferate in a desired shape or structure. To accomplish that, a shape needs to be determined, the scaffold material needs to have pores that allow cells to grow into, the scaffold material needs to be strong enough to support the growing cell structure throughout the growing process, and the material should not harm the cells that are trying to be grown. Further details of these principles are below.

2.2.1 Pore Size and Morphology

The size, shape, and amount of pores in a scaffold greatly affect its ability to grow new tissue. The size and shape of pores and the level of porosity also greatly affect the mechanical properties of the scaffold. [19] A scaffold with optimum cell viability will have a great reduction in mechanical strength when compared to a solid material, or even a scaffold with less porosity

or smaller pores. [20] [21] In one study by Yu et al, two different sizes of NaCl were used as a porogen to definitively determine the effects of porosity and pore size on the mechanical strength of bone tissue scaffolds. The NaCl was separated into two different size ranges of 212-355 μm (Group A) and 355-600 μm (Group B). The NaCl was mixed into the rest of the scaffold solution at ratios of 4:1, 1:1, and 1:4 (NaCl to scaffold solution). This allowed for different porosities for each group of NaCl as well as comparing pore size and porosity differences between the two NaCl groups. As can be seen in Figure 4, the porosity of the scaffold decreases as the ratio of NaCl in the scaffold decreases. Also, the porosity for Group A scaffolds is significantly less than the Group B scaffolds at the same NaCl ratio. As would be expected, the larger porogen corresponded to a larger pore size. [17]

A large number of interconnected pores is also desired for bone tissue scaffolds. These interconnections allow cells to grow within the entire scaffold and prevent an over accumulation of cells on or near the surface. An increase of the porogen content also increased the amount of interconnections in the scaffold. [19] [21] Furthermore, the use of HA in these scaffolds had an effect on the surface roughness in the pores. The larger pores had more HA exposed and therefore created a rougher surface. This rougher surface is desired for tissue scaffolds since the cells will bond more easily to a rougher surface. Finally, the size and amount of pores had an effect on both the

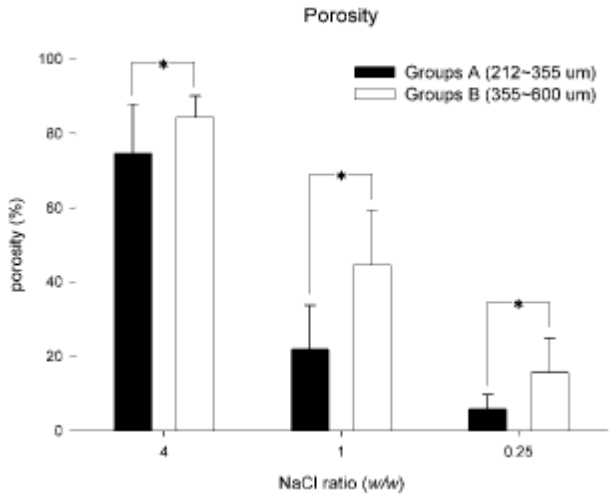

Figure 4: The porosities of the PCL-HA composites fabricated with two distinct sized porogen particles at various concentrations. Data collection and analysis were based on GE MicroCT system (*p < 0.01). **[17]**

tensile strength and the Young's modulus of these scaffolds. Figure 5 shows the results of tensile strength and Young's modulus for all of the tested scaffolds. For both of these mechanical tests, the increase of porogen decreased the strength of the material. All of the samples in the tensile testing behaved in the same manner with a linear-elastic increase in stress, followed by a plateau and finally a decrease in stress leading to the failure point. The size of porogen seemed to have opposite effects on the strength of the material when comparing tensile strength and Young's modulus. At the same porogen to polymer concentration, the Group B scaffolds had a higher tensile strength and a lower Young's modulus than the Group A scaffolds (except at 4:1 ratio where the Group B's Young's modulus is higher). [17]

The uniformity of the pore size and structure can also affect a scaffold's ability to grow cells. The pores of the scaffold need to be larger than a certain minimum size, with good interconnectivity between pores in order for the cells seeded onto the surface of the scaffold to permeate into the 3-D structure of the scaffold. The space occurring between the pores, sometimes called "windows", can also have affect the growth of cells if they are not of proper size or quantity. Problems that can occur with non-uniform pore size scaffolds are difficulty

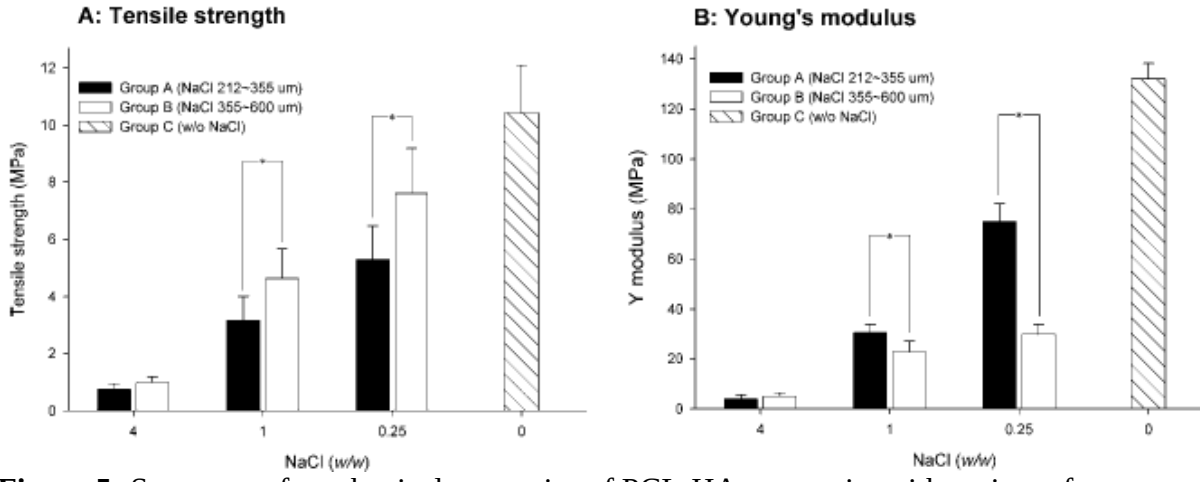

Figure 5: Summary of mechanical properties of PCL-HA composite with variety of porogen concentration and particles size (*p < 0.05). **[17]**

with reproducing results from experiments due to the random nature of non-uniform pore sizes, areas of smaller pores that would inhibit cell growth, and the general difficulty to pinpoint the optimum pore size for growing cells on scaffolds.

A study by Choi et al was performed to determine what effect scaffolds with non-uniform pore sizes had on the distribution of cells when compared to scaffolds with uniform pore sizes. Both sets of scaffolds were made from PLGA, had an average pore size of around 200 μm and were fabricated using the same process. Called inverse opal scaffolds, microspheres were created out of gelatin using a fluidic device and arranged into a cubic-closed-packed (ccp) lattice. The microspheres were interconnected with each other using a heat treatment for a polymer solution to then fill the void spaces of the microsphere structure. The microspheres are finally removed using a warm water bath after the polymer solution has solidified. SEM images for both the uniform pore scaffold and the non-uniform scaffold can be seen in Figure 6. The figure also shows the distribution of pore and window size for both types of scaffolds. The distribution of cells for

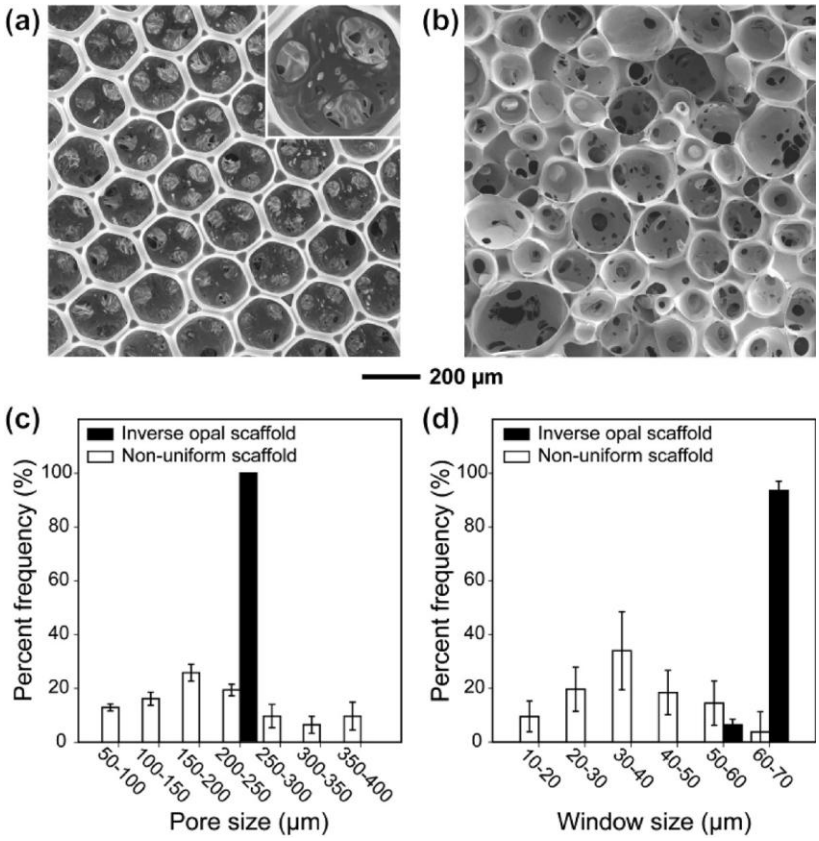

Figure 6: SEM images of (a) an inverse opal scaffold and (b) a nonuniform scaffold, and size distribution (c) pores and (d) windows (or the holes connecting adjacent pores) in each scaffold. **[22]**

the two types of scaffolds was compared. Cells were cultured on the scaffolds for 7 days. Micrographs of the stained nuclei of the cells were observed at the middle plane of the scaffolds. Visual and quantitative analysis of the micrographs both confirmed that there was a more uniform distribution of cells at the middle plane for the uniform pore scaffolds. [22]

There is a necessity to tailor the pores and morphology of the scaffold in correlation to the type of cells being grown on them. Interconnected structures of pores with rough surfaces are the most ideal due to large surface areas for transportation of cells as well as cell attachment. [17] [23] [24] [7] Larger pores allow for easier distribution of the cells throughout the scaffold so they don't collect and grow exclusively on the surface. Growth occurring only on the surface could cause a lack of oxygen and other nutrients to cells deeper within the scaffold and can lead to necrosis. [22] [24] Most studies have determined that the optimal pore size is between 200 and 600 μm. [17] [22]

2.2.2 Mechanical Strength of Bone Tissue Scaffolds

The most ideal bone tissue scaffold would have similar mechanical strength as the bone it is intended to replace. As mentioned previously, the size and amount of pores changes the material strength of the overall composite. Strong materials aren't inherently more damaging to the host tissue once placed in vivo; however, factors other than mechanical performance must be considered. If a composite that degrades as the new tissue is form is desired, a stronger composite may degrade at a slower rate depending on the factors that increased its strength (fewer or smaller pores, additives in the composite, etc.). In particular, a higher strength porous composite may be due to smaller or fewer pores which would have a negative impact on the growth and proliferation of new tissue cells throughout the entirety of the structure – potentially leading to necrosis. One of the goals of bone tissue scaffolding is to replace the defective bone

with the tissue scaffold as a temporary place holder while the new bone tissue grows. Obviously, for this reason, a scaffold weaker than the bone it is trying to replace can be detrimental to the host, as once placed in vivo further surgeries or other complications may result from mechanical failure of the structure.

2.2.3 Biocompatability

It is of the upmost importance that the bone tissue scaffold is biocompatible, meaning that any of the materials used in the composite would not have a negative impact on host tissue once in vivo. Obviously, using any material that would be toxic to the cells trying to be cultured or to any host cells the scaffold would interact with in vivo would not be ideal. There are a series of tests created by the International Organization for Standardization for testing the biocompatibility of materials. Some of these tests include in vitro cytotoxicity, degradation of ceramics, and ethylene oxide sterilization residuals. For a complete listing of these tests, reference ISO 10993.

2.3 Scaffold Components

The main component for a 3-D porous bone scaffold is a polymer. Many of these scaffolds are also biocomposites, meaning that the polymer matrix includes some type of filler. These fillers can be used to increase the mechanical strength of the scaffold, make the scaffold more osteoconductive, or add some other desired property to the scaffold (such as making it antibacterial). Successful 3-D porous scaffolds have been produced in previous studies and a few of them will be mentioned below.

2.3.1 Polymer

A polymer is the most commonly used matrix for bone tissue scaffolds, due to the various methods and techniques available for their fabrication. The wealth of existing knowledge and

prior studies for their application as a bone tissue scaffold makes them especially suitable. All of the polymers to be discussed here are thermoplastics meaning that they melt at high temperatures and solidify at cooler ones. All ways of forming thermoplastics can also be reversible.

PCL is a linear aliphatic polyester polymer that has been approved by the FDA for its use in drug delivery systems. [17] [25] Previous studies have shown PCL to be biocompatible in its use and ability to degrade in vivo. The rate of degradation for PCL is slower than other polymers due to its high crystallinity, giving more structure to the scaffold while the new bone tissue is growing. [17] [25] [5] [20] [26] The molecular formula of PCL is $(C_6H_{10}O_2)_n$ with the structure that can be seen in Figure 7. [27] Previous studies have shown that PCL is nontoxic to cells and is in particular biocompatible with osteoblasts, the primary cell in bone formation. [4] [28]

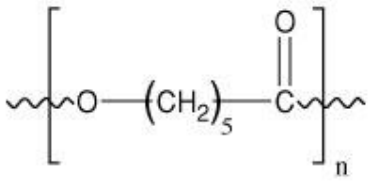

Figure 7: Molecular structure of polycaprolactone. **[27]**

Polylactide (PLA) is also an aliphatic polyester that can be naturally created from corn starch, sugarcane and other organic sources. There are two isomers of polylactide, d-lactide (PDLA) and l-lactide (PLLA). A third dl-lactide (PDLLA) is a synthetic blend of d- and l-lactide. Melt processing of PLA can be difficult because temperature and moisture have a high influence on the mechanical properties. [29] The molecular formula for PLA is $(C_3H_4O_2)_n$ and the molecular structure can be seen in Figure 8. [30] PLLA has a much longer degradation rate than PDLLA, but has a higher tensile strength. Co-polymer blends of materials like PCL and PLLA are sometimes used to try and achieve a balance of material strength to degradation. In one study, a blend of PCL and PLLA was used to make microporous

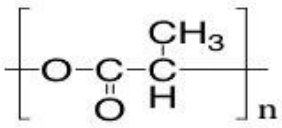

Figure 8: Molecular structure of polylactide. **[30]**

foams as a scaffold for hepatic cells. These two polymers were chosen due to the high permeation resistance and high retainability of yeast cells for PLLA and the low permeation resistance and low retainability of yeast cells for PCL. The blend allowed for sufficient hepatic cell growth into the microporous foams. [23]

A third aliphatic polyester commonly used in bone tissue scaffolds is polyglycolide (PGA). It is the simplest linear aliphatic polyester. PGA has a high crystallinity, making it insoluble in water and most organic solvents (which include acetone, dichloromethane, and tetrahydrofuran). The molecular formula for PGA is $(C_2H_2O_2)_n$ with a molecular structure that can be seen in Figure 9. [30]

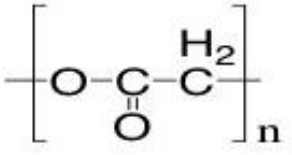

Figure 9: Molecular structure of polyglycolide. **[30]**

While PGA has a high tensile strength and modulus, the material degrades quickly. [29] As mentioned earlier, co-polymerization between PCL, PLA, and PGA is common when developing bone tissue scaffolds.

2.3.2 Hydroxyapatite

The molecular formula for hydroxyapatite (HA) is $Ca_5(PO_4)_3(OH)$. It is a ceramic material and therefore very brittle. It is naturally found in bone and is consequently a common reinforcement to polymers used for bone tissue scaffolding. When used in a composite with polymers like the ones mentioned in the previous section, the brittleness of the HA can balance out with the flexibility of the polymers. [17] While the polymers used are not osteoconductive, HA is – meaning that it helps with the growth of osteoblasts in the scaffold. [4] [5] [6] [7] There are two basic varieties of HA: synthesized and natural. Effectively, synthesized HA uses a bottom up approach, while natural HA is a top down manufacturing process. [31]

Natural hydroxyapatite is collected by taking bone (for example cow bone), and burning

the excess tissue, fat, marrow, etc. from the bone at 700 C, in a process similar to cremation. The left over hydroxyapatite maintains the shape of the original bone, but is much lighter and completely white in color. The hydroxyapatite can then be ground to the size desired (through milling, mortar and pestle, etc.).

In one study by Calandrelli et al, natural and synthetic HA filled PCL was created to test the tensile properties of the samples and the proliferation of the cells on them. Comparisons were made between the natural HA filled PCL, synthetic HA filled PCL, and pure PCL. The natural HA was heated at 450 C for an unspecified amount of time to remove all organic material. Synthetic HA whiskers were created using the following method:

- $Ca(NO_3)_2$ X $4H_2O$ and $(NH_4)_2HPO_4$ were dissolved in a mixture of methyl cellulose and water.
- NH_4OH was added and the solution was stirred for 3 hours at 60-70 C.
- Precipitates were collected by filtering/centrifugation and washed.
- After being dried overnight at 100 C, the HA powder was calcined for 6 hours at 1000 C.
- The powders were then ground and mixed with K_2SO_4 and heated to 1190 C for 3.5 hours.
- Once cooled, the whiskers were separated from a solid mass and washed in hot water and dried overnight at 100 C.

a)
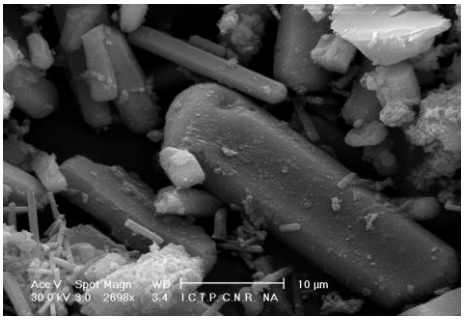

b)
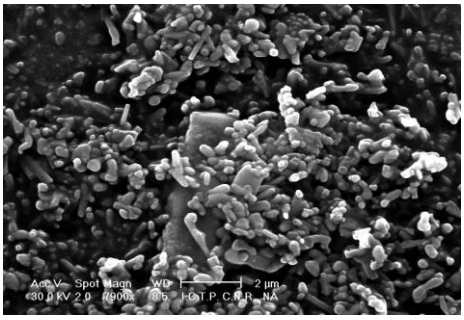

Figure 10: SEM micrographs of a) synthetic HA whiskers (2700x) and b) natrual HA powder (2000x). **[32]**

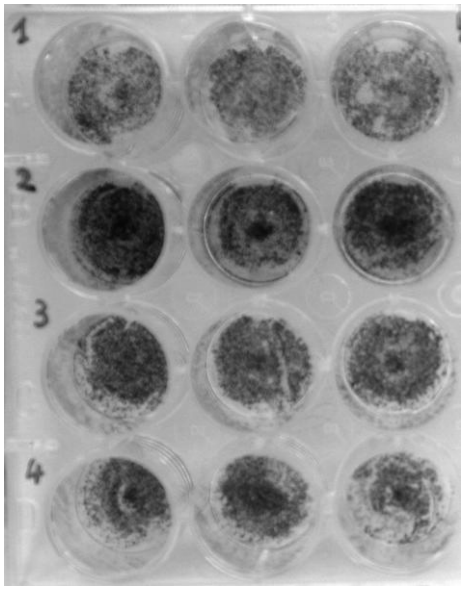

Figure 11: MTT assay of MSC cultured samples (1 = 10 wt% natural HA, 2 = 10 wt% synthetic HA, 3 = 20 wt% natrual HA, 4 = 20 wt% synthetic HA). **[32]**

SEM micrographs of the synthetic and natural HA particles can be seen in Figure 10. A screw extruder that was specifically designed for mixing extruded the PCL and HA composite samples. The samples were subjected to tensile tests and a MTT assay using mesenchymal stem cells (MSC). The tensile tests showed that while the natural HA powder had improved Young's modulus, the synthetic HA whiskers had a higher peak stress and strain. All samples with HA had higher tensile test results than pure PCL. Results of the MTT assay can be seen in Figure 11. As can be seen, the 10 wt% synthetic HA whisker sample was the most successful at culturing MSC, but all of the HA samples had cell growth and did better than pure PCL. This shows that while there are differences between synthetic and natural HA, they both improve the mechanical and biological properties of the polymer matrix. [32]

Another study performed by Lao et al, HA particles were synthesized using chemical coprecipitation through aqueous solution. Like the previous synthetic HA method, $(NH_4)_2HPO_4$ was used but was instead dropped into a $CaCl_2$ to achieve a final Ca/P molar ratio of 1.67, the same molar ratio in HA's molecular formula. Precipitates were formed under agitation and calcinated at 900 C for 4 hours. The particles were finally ultrasonicated to disperse the granules to spherically shaped particles with an average size of 266.6 ± 7.3 nm. SEM micrographs of the HA particles before and after ultrasonication (a and b, respectively), TEM image, and EDS can be found in Figure 12. As seen in Figure 12(d), the major elements in the HA particles are

phosphorous and calcium with a ratio of Ca/P of 1.634, very near the theoretical 1.67 that was desired. [8]

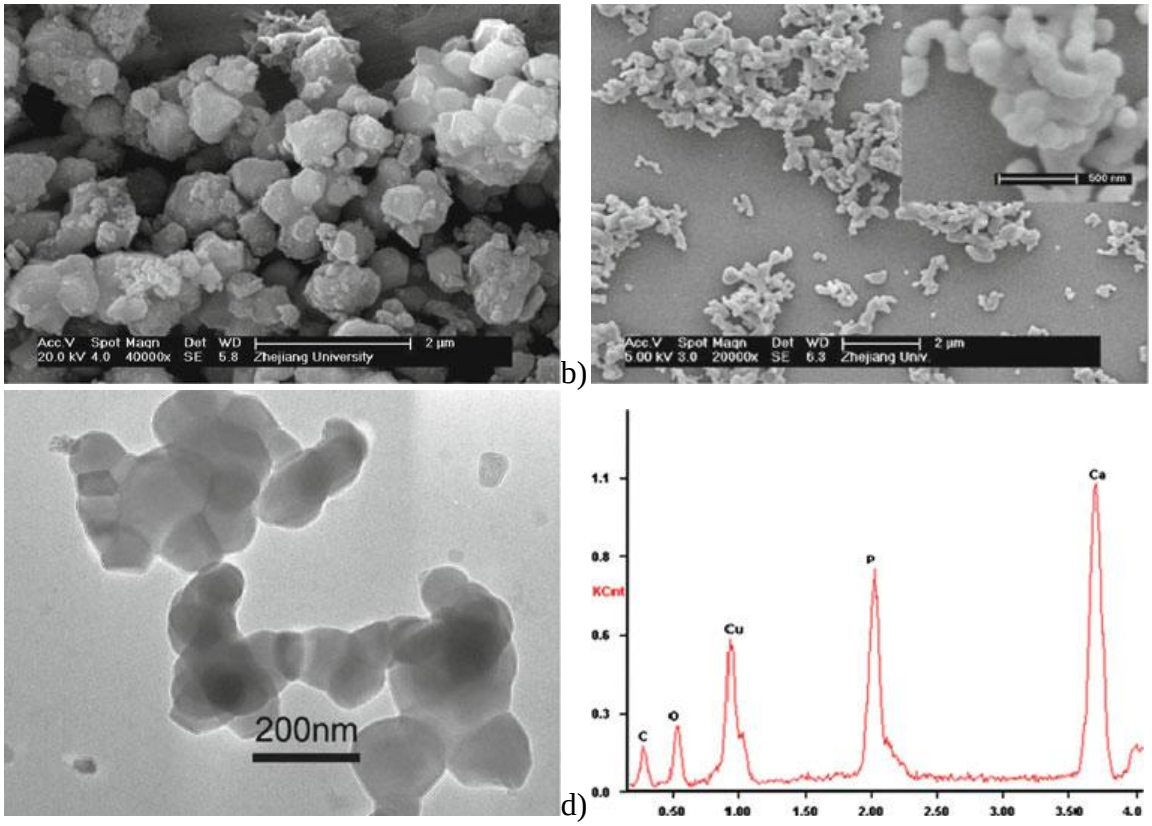

Figure 12: SEM micrographs of HA particles before (a) and after (b) ultrasonication, c) TEM image of HA particles, d) EDS of HA particles after ultrasonication showing the atomic ratio of Ca/P. **[8]**

2.3.3 Gentamicin

Gentamicin (also known as gentamicin sulfate) is an aminoglycoside antibiotic used to treat bacterial infections. Aminoglycosides are molecules where some portion of it is made of an amino-modified sugar. Other aminoglycoside antibiotics include streptomycin, ribostamycin, and verdamicin. Gentamicin is used to treat many types of bacterial infections, but is most often used for gram-negative bacteria. Gram-negative bacteria are ones that do not retain crystal violet dye. This is due to a protective wall (that is not present in gram-positive bacteria) that resists the dye. This protective wall also makes these bacteria more resistant to antibodies. Some examples of gram-negative bacteria are escherichia coli (E. coli), salmonella, and legionella. Gentamicin

has interest for use in orthopaedic surgery and other biomedical applications because it is one of the few heat-stable antibiotics and remains active even after going through an autoclaving process.

2.3.4 Manufacturing Methods

There are many ways to introduce pores into a polymer. Below are a few of the options.

Salt leaching is a method of creating 3-D porous structures by using NaCl salt as a porogen. Typically, salt is evenly dispersed in a polymer and solvent mixture through high levels of mixing such as through sonication. After the solvent in the mixture evaporates and the polymer and salt blend is solidified, the salt is dissolved using water. As mentioned previously, the size and quantity of the pores can be controlled by adjusting the size and amount of salt. [7] A potential problem that can arise with this technique would be that the polymer and solvent mixture is too laminar and the salt can accumulate unevenly at the bottom of the final scaffold once the solvent has evaporated. A highly viscous slurry of materials is desired after the mixing with salt. [17]

Solvent leaching uses a similar concept for creating pores as salt leaching. The main biocompatible polymer is combined in an immiscible polymer blend with a "sacrificial" polymer that is then leached out with solvent creating pores in the space that once had the sacrificial polymer. The main benefit to using solvent leaching is while other processes to induce pores like salt leaching and gas foaming can be fine tuned to adjust pore size and quantity, an interconnection of the pores cannot be guaranteed. As can be seen in Figure 13, the pores are interconnected but the size and structure of the pores are not uniform. In one study, 50:50 and 70:30 wt% blends of poly-L-lactic acid (PLLA) and polystyrene (PS) were created by mixing at 60 rpm and 200 C for 10 minutes ensuring a homogenous mixture of the two polymers. Once

the polymer blend had been formed into the desired shape, a solvent that would affect only the sacrificial polymer (in this case cyclohexane) was used to remove the PS. The resulting porous scaffolds had larger pores for the 50:50 than the 70:30 blend [24].

Gas foaming is a process that introduces bubbles into the polymer structure by saturating the polymer with an inert gas, such as CO_2. These bubbles form the pores in the finished scaffold. This process can be used with salt or solvent leaching by combining a sacrificial material into the polymer before the gas foaming process. The sacrificial material is leached out through the typical methods after the pores from gas foaming have formed. In one study by Salerno et al, PCL was mixed with a thermoplastic gelatin (TG) and then subjected to gas

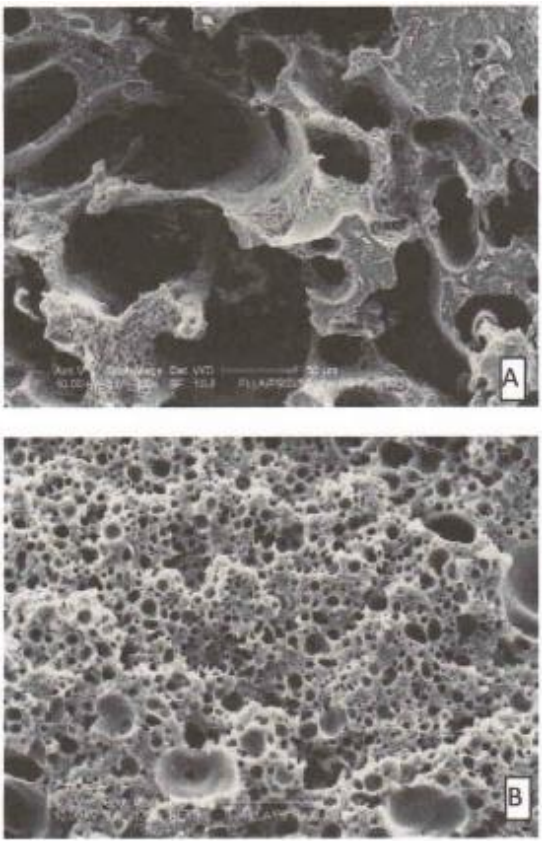

Figure 13: SEM micrographs of the continuous microporous structure after solvent leaching of (A) 50:50 wt% PLLA to PS and (B) 70:30 wt% PLLA to PS **[24]**.

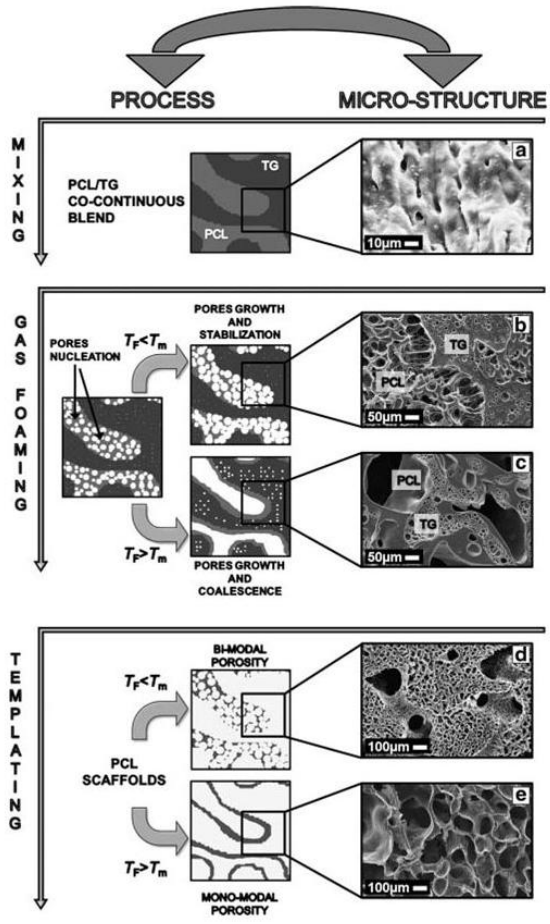

Figure 14: Gas foaming process. **[19]**

foaming using a gas mixture of 4/1 vol% of N_2/CO_2. Two types of samples were created during the foaming, one where the polymer blend was below the melt temperature of PCL during the foaming and one where the polymer blend was over the melt temperature of PCL. Figure 14 shows the process used and the evolution of the micro-structure of the scaffold using SEM micrographs. The pores created by the gas foaming were much smaller when the polymer blend was below the melt temperature of PCL. This resulted in small pores connected between larger pores that were created by the removal of the TG. When the polymer blend was higher than the melt temperature of PCL, the individual pores created by the gas foaming combined to create larger pores that were similar to size as the pores created by the removal of the TG. [19]

There are many ways to form the scaffold, in particular when using the salt leaching or solvent leaching methods where the desired final shape of the scaffold matches the initial shape produced. Among them are placing the polymer mixture in a cavity that would provide the final shape of scaffold desired. This technique is capable of producing circular, rectangular or even more complex geometries. Possible manufacturing methods include compression molding (where an already solidified polymer or polymer blend is heated and pressed into the desired mold), and injection molding. Injection molding is quite similar to compression molding, but is capable of molding the polymer into more complex shapes [28]. The solidified polymer or polymer blend is cut into pieces that would be able to fit into the hopper for

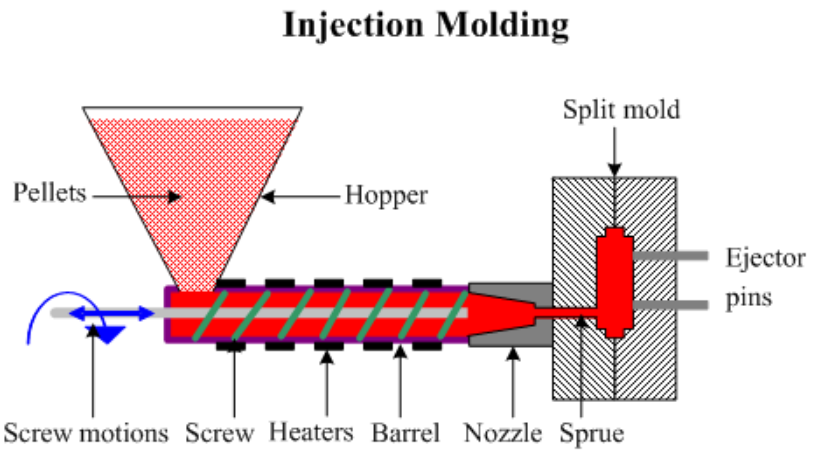

Figure 15: Horizontal injection molding configuration. **[33]**

the injection molding machine. The hopper holds all of the solid material as it is heated to reduce the viscosity of the polymer. A pressurized ram (for vertical machines) or a rotating auger (for horizontal machines) pushes the polymer into the opening that leads to the mold. A schematic of a horizontal injection molding machine can be seen in Figure 15. [33] The mold is typically heated to ensure the polymer fills the entire cavity and does not start solidifying too soon. Once cooled, the porous shape can be achieved by leaching out the salt or other sacrificial material. The main benefit of using injection molding for scaffolds is the ability to form complex shapes, that can then be utilized for the fabrication of bone tissue scaffolds. [28] [34]

Electrospinning is a process to make micro- or nano-sized fibers of the intended polymer. [5] [35] Furthermore, the fibrous structure that is achieved through electrospinning resembles the extracellular matrix of bone. [8] [9] The main parameters occurring during electrospinning can be seen in Figure 16. [36] A polymer and solvent solution is transferred to a syringe that is placed in a machine that ensures an even flow rate of the solution from the syringe. An electric field is then introduced between the tip of the syringe and a collection target a desired set distance away. The field is created by introducing either a positive or negative electrical charge to polymer solution at the tip of the syringe. [37] This is typically done by either using an electrically conductive metal syringe tip, or wiring some copper wire through the syringe tip that would be able to electrically charge

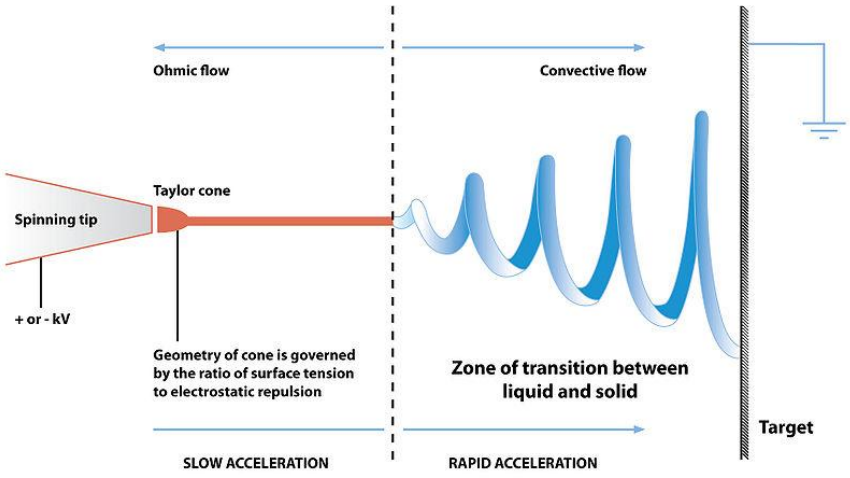

Figure 16: Schematic of the electrospinnning process. **[36]**

the polymer solution near the tip of the syringe. Obviously, it must still be connected to the electrical source outside of the syringe. [35]

The collection target is either grounded or is itself introduced to a smaller and oppositely poled electrical charge. The applied potential of the electrical field is the difference of electrical charge between tip of the syringe and the collection target. The electric field causes the polymer mixture to rotate which results in the mixture thinning the longer it rotates. The final result is a non-woven mat of fibers, ideally of even distribution and diameter. These mats of fibers have a high surface area, are flexible and are naturally porous. The morphology of the fibers can be controlled by changing different aspects of the process including viscosity of the polymer solution, strength of the electrical field, flow rate of the polymer from the syringe and distance from the tip of the syringe and the target. [37] The solution of the polymer and solvent needs to have a sufficiently laminar flow to ensure that it flows evenly through the syringe without a possibility of clogging; however, if the viscosity is too laminar, the solution could break up within the electric field and spray towards the collection target instead of forming one consistent fiber. Viscosity can be adjusted by increasing or decreasing the ratio between the polymer and solvent. An increased flow rate of the polymer leaving the tip of the syringe would result in thicker fibers. Conversely, a slower flow rate would produce thinner fibers. Finally, the greater the distance between the syringe tip and the collection target, the thinner the resulting fibers will be due to the increased spinning that would occur in the electric field. [35]

Rapid prototyping, also known as 3-D printing, is one of the most likely candidates for the future of creating porous bone scaffolds. A completely porous and interconnected pore scaffold can be designed on a CAD programming software, and the resulting scaffold can immediately be created out of a desired polymer. Rapid prototyping works by fabricating each

layer of the scaffold at a time building up to the final product. The layers are formed by using a laser to cure a thermoset polymer or a thin nozzle is used to distribute melted thermoplastic polymers. The main setback currently for using rapid prototyping to create scaffolds is that they have too low of a resolution to create pores small enough to ensure proper cell growth.

CHAPTER 3

EXPERIMENTAL PROCEDURE

The main materials used for this thesis were PCL, Dimethylformamide (DMF), Dichloromethane (DCM), gentamicin, and natural HA. The PCL pellets were purchased from Scientific Polymer Products, Inc and have a MW of 70,000. N,N-Dimethylformamide was purchased from Arcos Organics. Dichloromethane was purchased from Alfa Aesar. Finally, gentamicin sulfate powder was made by National Fish Pharmaceuticals. The materials used can be seen in Figure 18. Natural HA was obtained in the lab using the same process outlined in the literature review (cremation in an oven at 700 C for 2 hours). The resulting HA was then ground into a fine powder, via mortar and pestle, which allows it to pass through the tip of the electrospinning needle without becoming clogged. This process is shown in Figure 21. Finally, SEM and Energy-Dispersive X-Ray Spectroscopy (EDS) analysis was performed.

15 wt% of PCL was dissolved in a 50:50 wt% DMF: DCM mixture to make a PCL solution. 0, 5, 10, and 20 wt% of HA and 0, 5, and 10 wt% of gentamicin were mixed into the PCL solution. All materials were weighed on a Mettler Toledo XS64 Analytical Balance, which can be seen in Figure 17. The final solution was placed in a Fisher Scientific FS60D sonic bath for 5 minutes and then allowed to mix on a Corning analog stir plate, shown in Figure 19, which was heated to approximately 60 C and a speed of 450 rpm. The

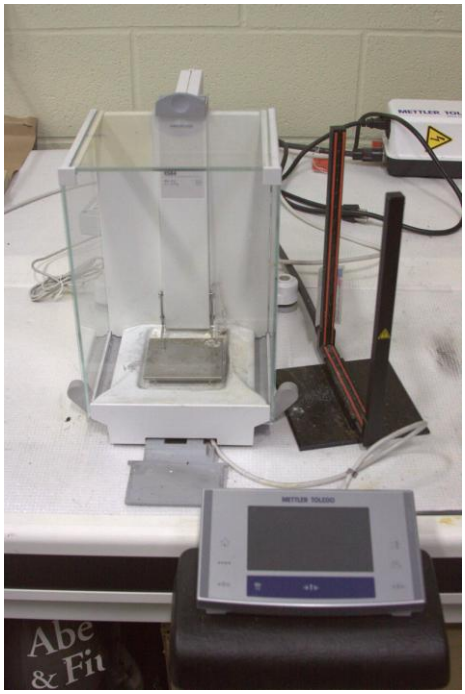

Figure 17: Mettler Toledo XS64 analytical balnce.

solution was allowed to mix overnight for up to 24 hours.

a) 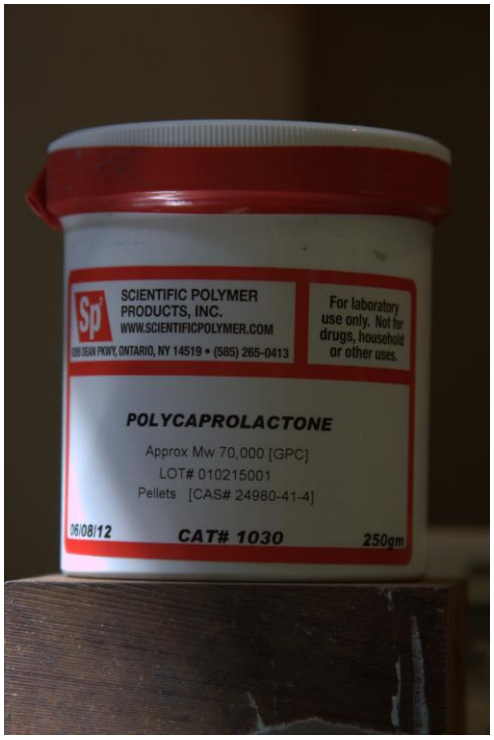

b) 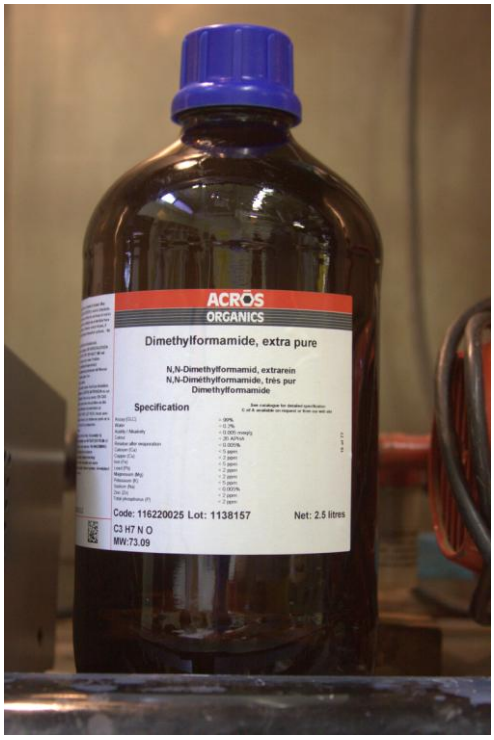

c) 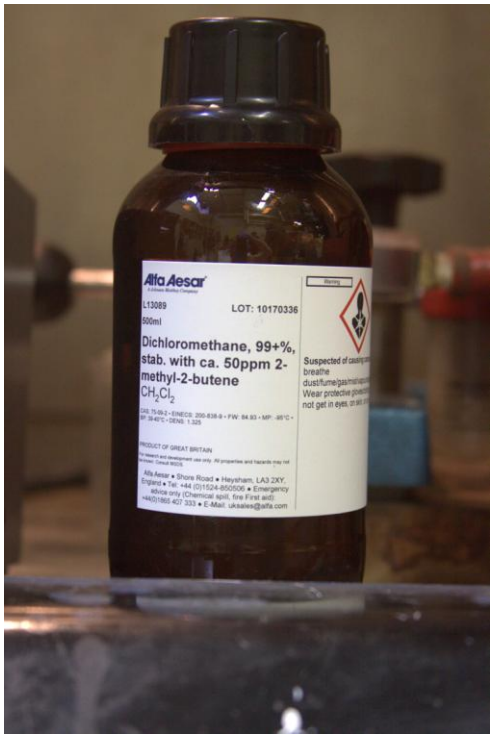

d) 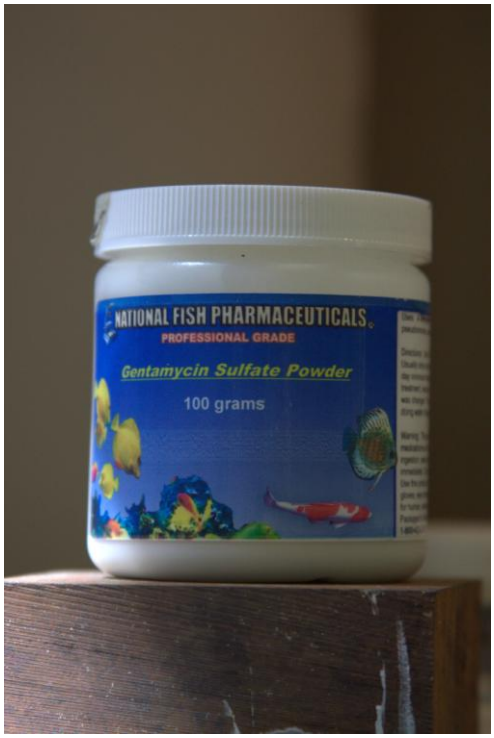

Figure 18: Materials used in this study. a) Polycaprolactone, manufactured by Scientific Polymer Products, b) DMF, manufactured by Acros, c) DCM, manufactured by Alfa Aeser, and d) gentamicin, manufactured by National Fish Pharmaceuticals.

Figure 19: Corning analog stir plate.

Figure 20: Fisher Scientific sonic bath.

a)

b)

c)

d)

Figure 21: Preparation of HA: a) removal of organic material in the furnace, b) piece of HA in a mortar and pestle, c) HA crushed into a fine powder which coats the mortar walls, and d) the resulting powder after being scraped from the mortar walls.

The fully mixed solution was transferred into a 10 mL syringe and placed in a KD Scientific syringe pump with a flow rate of 2 mL/hr. Each syringe was modified by poking a hole near the base of the syringe, inserting a copper wire into the hole with one end still on the outside of syringe and the other end inside the syringe towards the tip of the needle. Epoxy

(manufacturer's identification is "Loctite Epoxy Plastic Bonder") was used to ensure a tight seal between the copper wire and the syringe, such that no leaks would occur. An image of the final prepared syringe can be seen in Figure 22. The copper wire was connected to a power supply with a voltage of 21.5 kV from a Spellman SL 10 compact HV power supply. Aluminum foil was wrapped around a collection grid and was grounded and placed 25 cm away from the tip of the needle. The foil was sprayed with mold release agent to ease the removal of the fibers. The whole electrospinning process was carried out in ambient conditions; the electrospinning equipment can be seen in Figure 23. After all of the fibers were collected, they were dried for at least 48 hours before being collected off of the aluminum foil. Each mat of fiber was stored separately in a single layer between two sheets of paper towel and kept in a zipper top plastic bag. Electrospun sheets, shown both before and after removal from the target, are shown in Figure 24. SEM micrographs were taken of the nanofiber mats.

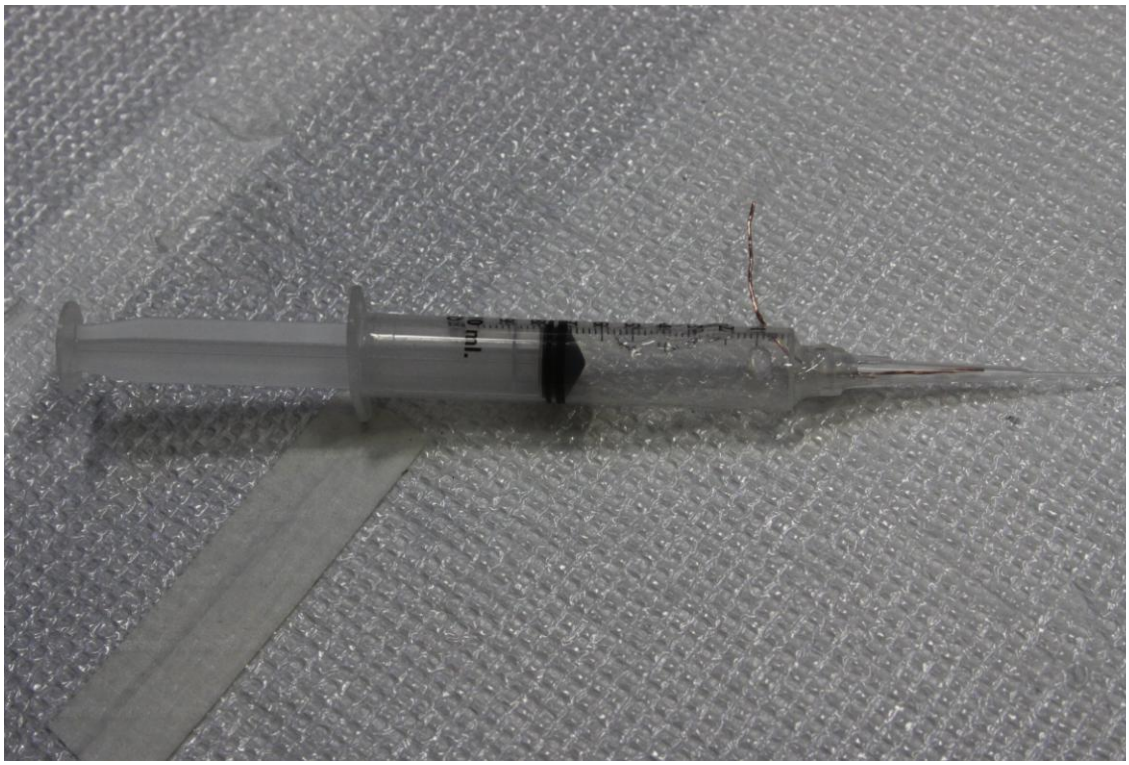

Figure 22: Prepared syringe for electrospinning.

a)  b) 

c) 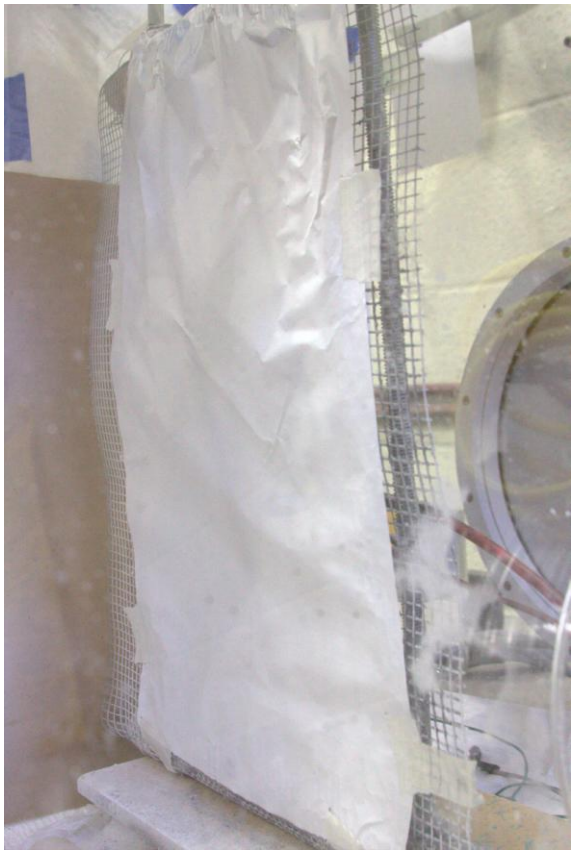 d) 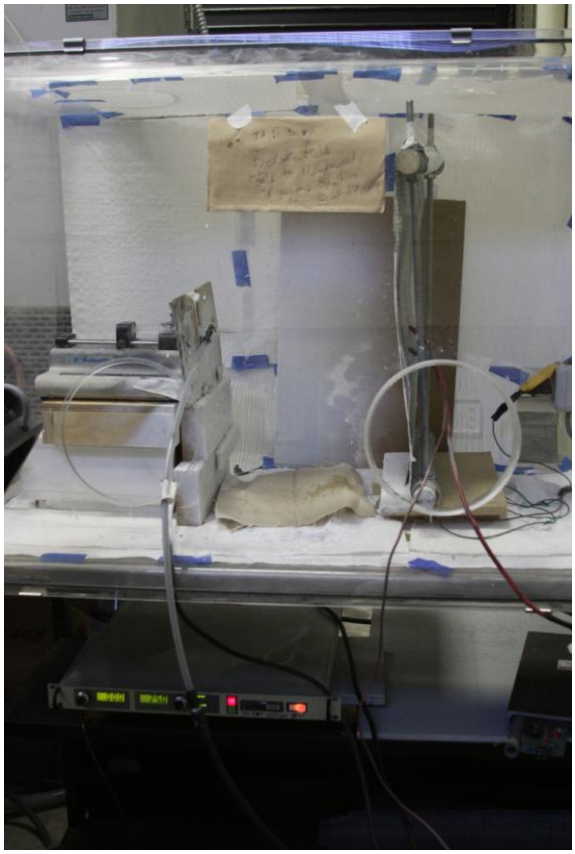

Figure 23: Components of electrospinning including a) syringe pump, b) power source, c) collection grid with aluminum foil, and d) the entire set-up.

Anti-bacterial susceptibility tests were performed using a process that has a similar methodology to the Kirby-Bauer Disc method. An agar and lysogeny broth (LB) medium solution was mixed together and placed into 10 cm diameter petri dishes. These dishes were placed in an autoclave to allow the agar to harden. E. coli was cultured and 200 μL of the bacteria was diluted with

2000 μL of LB solution. 200 μL of the diluted bacterial solution was placed and spread evenly in each prepared petri dish. Three discs, approximately 0.75 cm in diameter, were cut from each nanofiber mat, using the tool shown in Figure 25a.. Three rows of three samples of anti-bacterial nanofiber were placed in each petri dish resulting in 9 samples in each dish, as shown in Figure 25b. Each petri dish was incubated to encourage bacteria growth and photos were taken for up to five days.

a)  b) 

Figure 24: Electrospun fiber a) collected on aluminum foil and b) removed and placed on a paper towel.

a)  b) 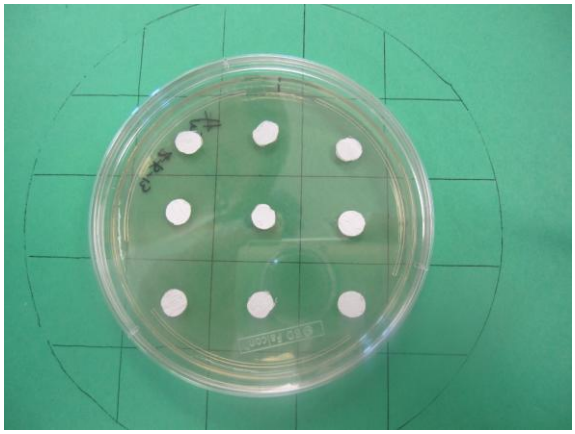

Figure 25: Biological testing set-up with a) tool used to uniformly cut material samples and b) day zero configuration of test samples.

CHAPTER 4

RESULTS AND DISCUSSION

SEM micrographs and EDS analysis of the natural HA can be found in Figure 26. When comparing the SEM micrograph of Figure 26 to Figure 10, the HA particles are of similar size and morphology as those seen in previous works. The EDS found in Figure 26 has similar peaks in Phosphorous and Calcium to those found in Figure 12. Furthermore, the atomic ratio of Ca to P from the numbers that can be found in Figure 26 is 1.70, which is quite close to the theoretical ratio of 1.67 and similar to the Ca/P atomic ratio of the synthetic HA calculated from Figure 12. These results confirm that the particles derived from the cow bone can indeed be classified as HA.

SEM micrographs for 0% HA, 0% gentamicin; 20% HA, 0% gentamicin; 0% HA, 10% gentamicin; and 20% HA and 10% gentamicin are shown in Figure 27. As can be seen in (b) and (d) of Figure 27, there are raised nodules in the fiber that indicate the presence of HA particles. This confirms that the inclusion of HA did not fail during electrospinning, due to a material clog in the syringe, or other failure. Measurements of the diameter of the fibers were taken from the SEM micrographs and had an average of 142.4 nm ± 62.96 nm. This confirms that the produced fibers were on the nano-scale. In a study done by Lao et al, PLGA/HA scaffolds were also created via electrospinning. The average diameter of these fibers was 266.6 ±7.3 nm and the SEM images of the fibers can be seen in Figure 28. Although, the fibers produced in their study are of a greater diameter than those presented in this study, the standard deviation is much smaller. The variation in diameter of the fibers is not ideal; however, the root cause of this variation is unknown, and there were no adverse impacts to the biological tests conducted as part of this study. When comparing the SEM images of their PLGA/HA nanofibers to the fibers in

Figure 27, it can be seen that the PLGA/HA nanofibers also had the raised nodules indicating the presence of HA in the nanofibers. [8]

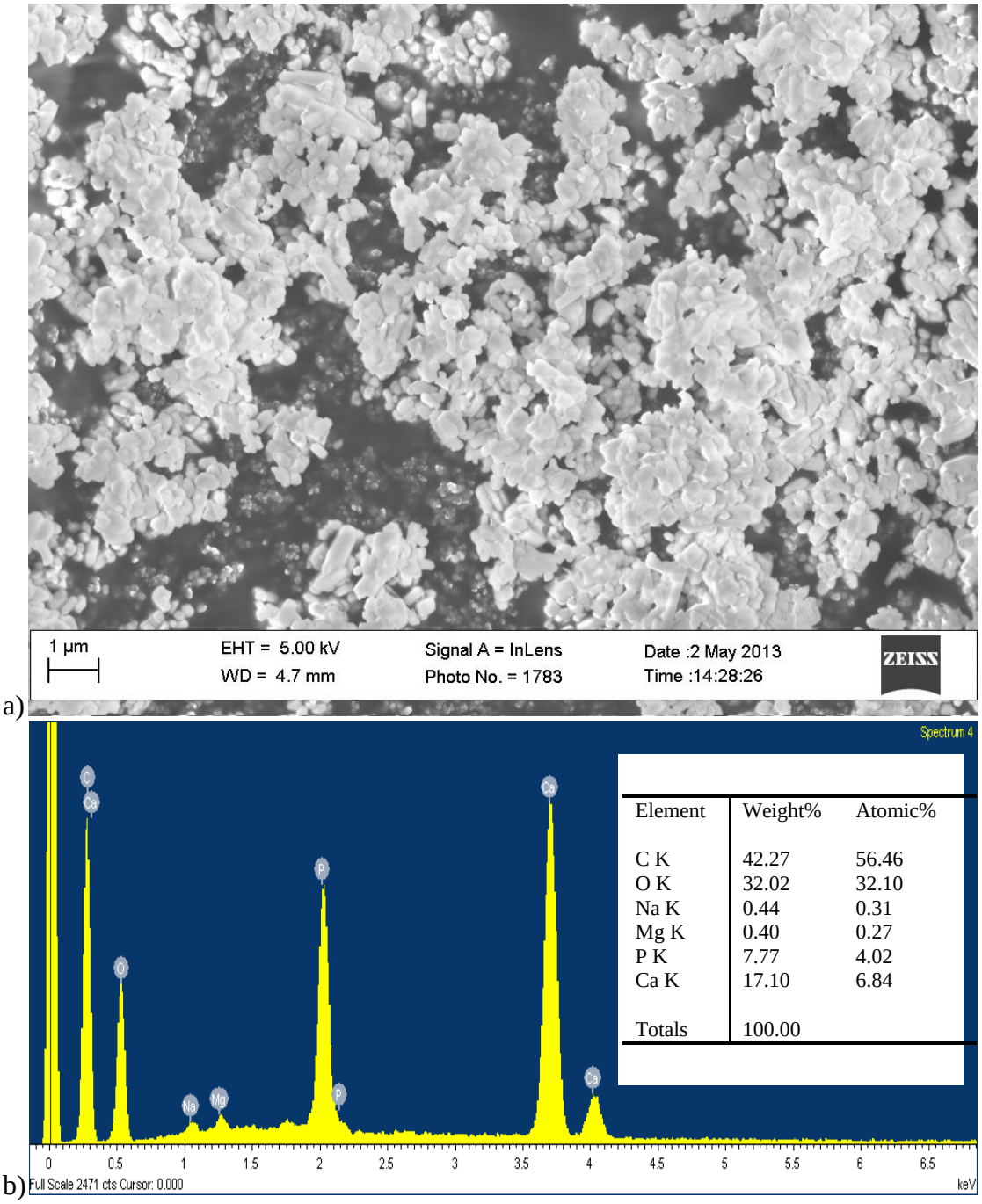

Figure 26: SEM micrograph (a) and EDS (b) of the natural HA.

This shows that this experiment has results similar to previous studies. The formation of beads in the nanofibers is not ideal and a study by Liu et al determined a few methods to eliminate the

presence of beads in electrospun nanofibers. Firstly, they used Poly(butylene succinate) (PBS) as their polymer and used many different types of solvents. The reason to using various solvents was because they were trying to determine an ideal solvent mixture balance that would form the least amount of beads. They came up with a solution that a mixture of two different solvents formed fewer beads than a single solvent, which corresponds to this study's use of a mixture of DCM and DMF for the solvent. Secondly, the concentration of polymer was adjusted from 11 to 17 wt% using the ideal solvent mixture found earlier (7:3 w/w of chloroform and 2-chloroethanol, respectively) and found that while the number of beads decreased from polymer concentrations of 11 to 14 wt%, no beads were formed at a polymer concentration of 16 wt% or higher. This study had a polymer concentration of 15 wt% which is a comparable percentage to what Liu et al used to achieve fibers with no beads. Finally, LiCl was added to the polymer mixture. The addition of the salt reduced the number of beads with the assumption being that the salt increases the electric conductivity of the polymer solution and improves the electrostatic forces. [38] This study didn't have any salts added to the polymer solution. Since the polymer concentration in this study was similar to 16 wt% polymer concentration that Liu et al used and many beads were formed in the fiber, it appears that the addition of salt, the mixture of solvents, or even the types of solvents led to the formation of beads.

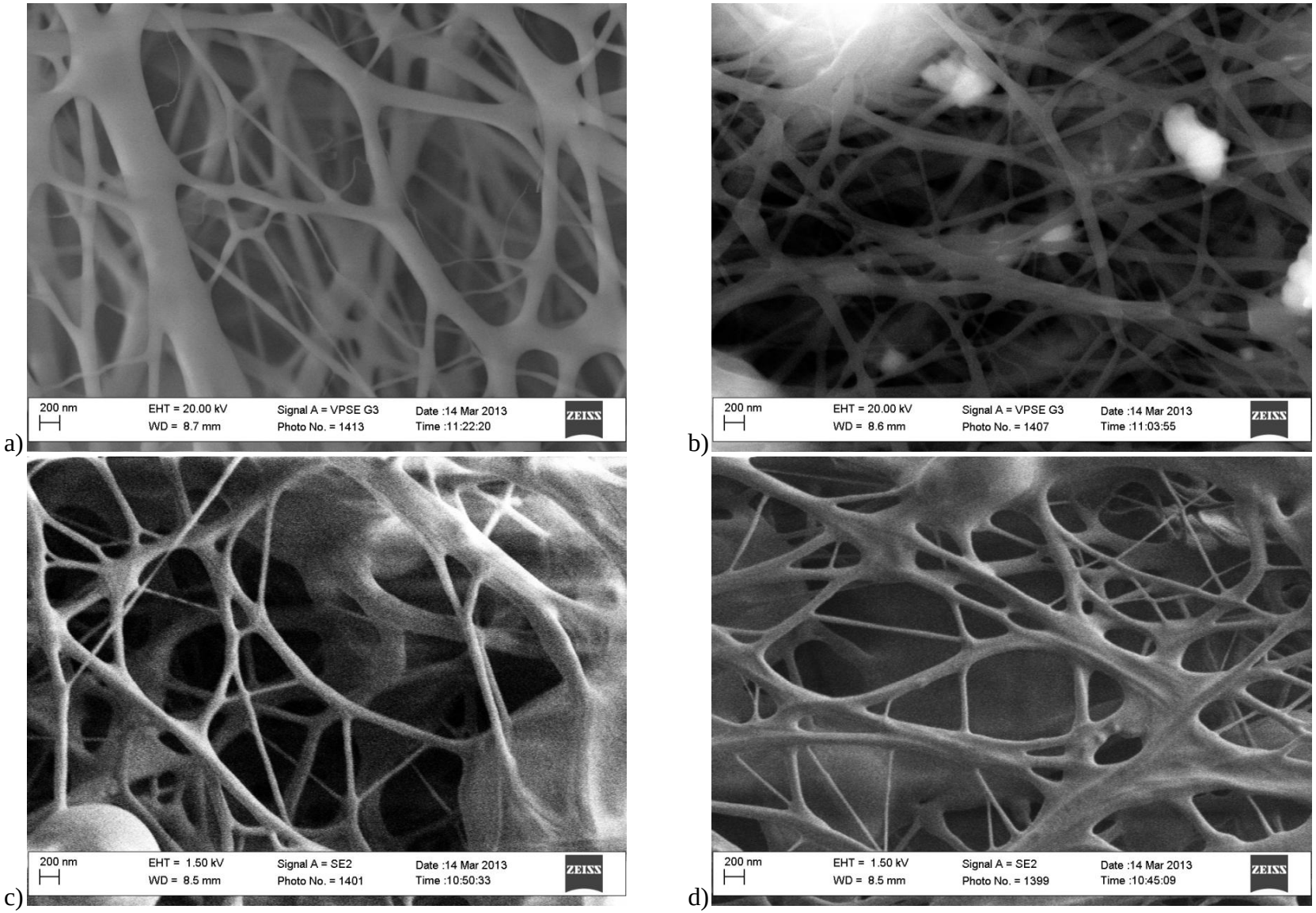

Figure 27: SEM micrographs of nanofiber PCL mats with added materials of a) 0% HA and 0% Gentamicin, b) 20% HA and 0% Gentamicin, c) 0% HA and 10% Gentamicin, and d) 20% HA and 10% Gentamicin.

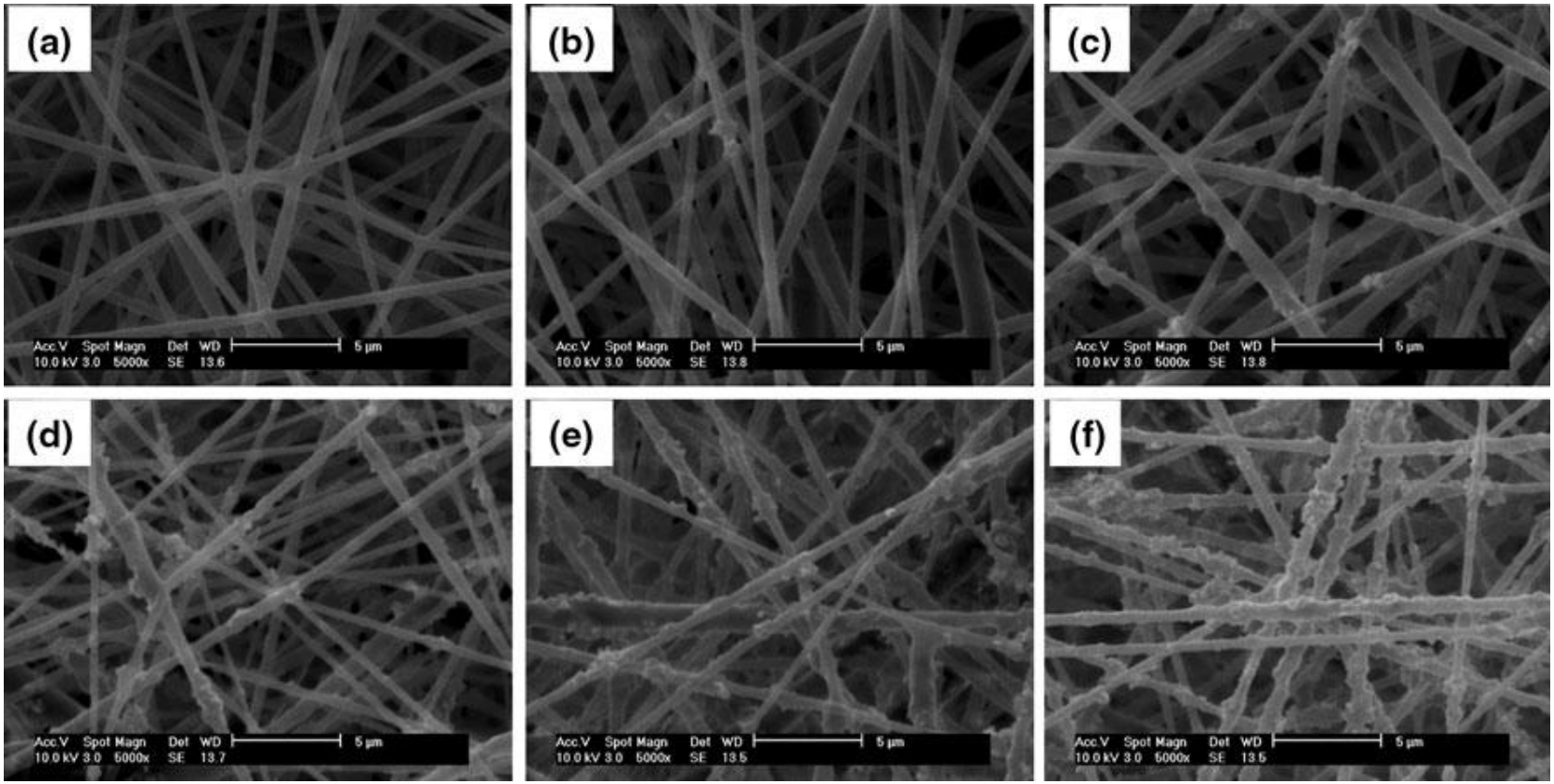

Figure 28: SEM images of PLGA with a) 0% HA, b) 0.5% HA, c) 2.5% HA, d) 5% HA, e) 10% HA, and f) 15% HA. **[8]**

During biological testing, all of the 0% gentamicin samples and 20% HA samples had pictures taken on day 1, 2, and 5 after initial culture on the petri dish. All other samples had pictures taken on day 1, 3, and 4 after initial culture. These pictures can be found in Figure 29 through Figure 40. Figure 29 through Figure 31 show samples of 0% HA, 0% gentamicin; 5% HA, 0% gentamicin; and 10% HA and 0% gentamicin on the first, second and fifth day after initial culture, respecitvely. Since all of these samples do not have gentamicin, the bacteria grows all the way to the edge of each sample. These results are excellent and show that any zone of inhibition that would be seen in later samples are due only to the gentamicin found in the nanofibers and not from any other source.

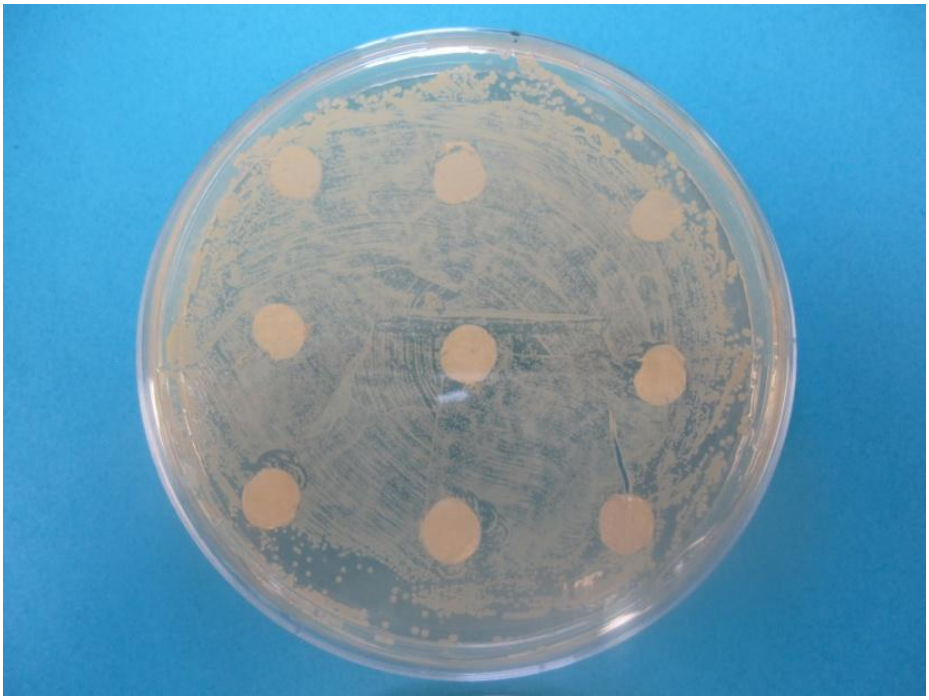

Figure 29: Biological results after 1 day. Top row are samples with 0% HA and 0% Gentamicin, middle row are samples wtih 5% HA and 0% Gentamicin, and bottom row are samples wtih 10% HA and 0% Gentamicin.

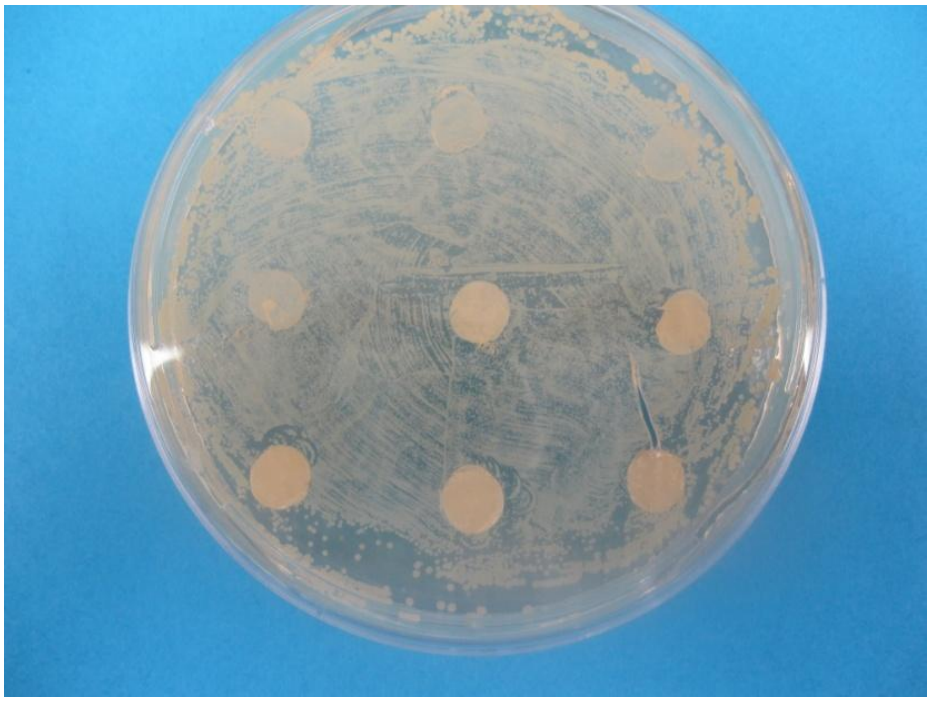

Figure 30: Biological results after 2 days. Top row are samples with 0% HA and 0% Gentamicin, middle row are samples with 5% HA and 0% Gentamicin, and bottom row are samples with 10% HA and 0% Gentamicin.

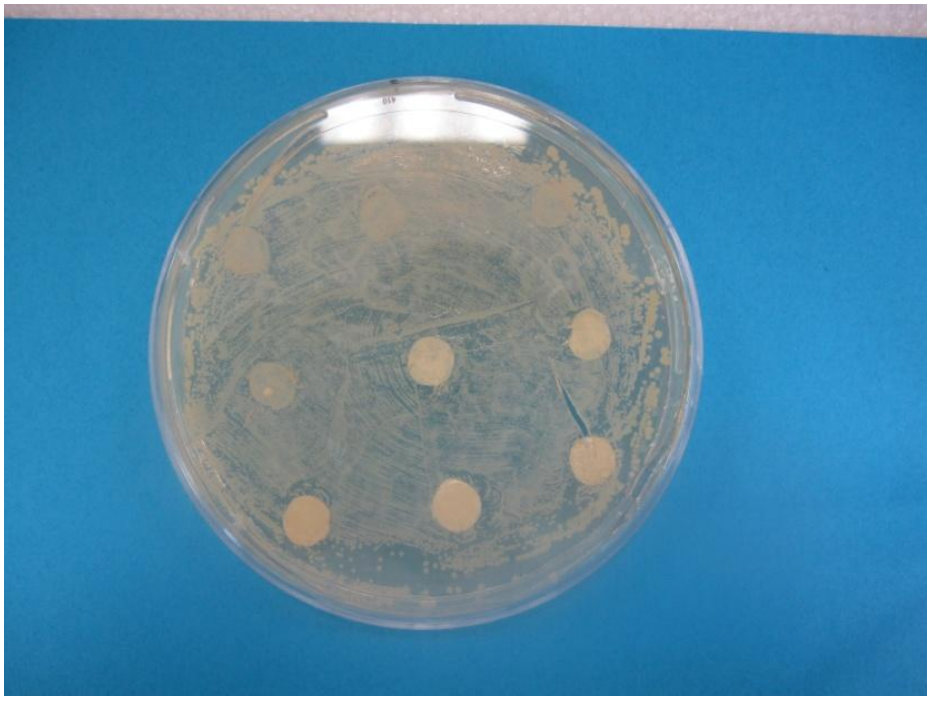

Figure 31: Biological results after 5 days. Top row are samples with 0% HA and 0% Gentamicin, middle row are samples with 5% HA and 0% Gentamicin, and bottom row are samples with 10% HA and 0% Gentamicin.

Figure 32 through Figure 34show samples of 20% HA, 0% gentamicin; 20% HA, 5% gentamicin; and 20% HA, 10% gentamicin after one, two, and five days respectively. Like the other 0% gentamicin samples, the 20% HA, 0% gentamicin sample has bacteria growing completely to the edge of the sample. The 5% and 10% gentamicin samples both have zones of inhibition surrounding the samples which means that the gentamicin is stopping the bacteria growth. Also, it can be seen that the 10% gentamicin samples have larger zones of inhibition than the 5% samples as expected. Finally, there is no discernable size difference in the zone of inhibition for each sample between different days.

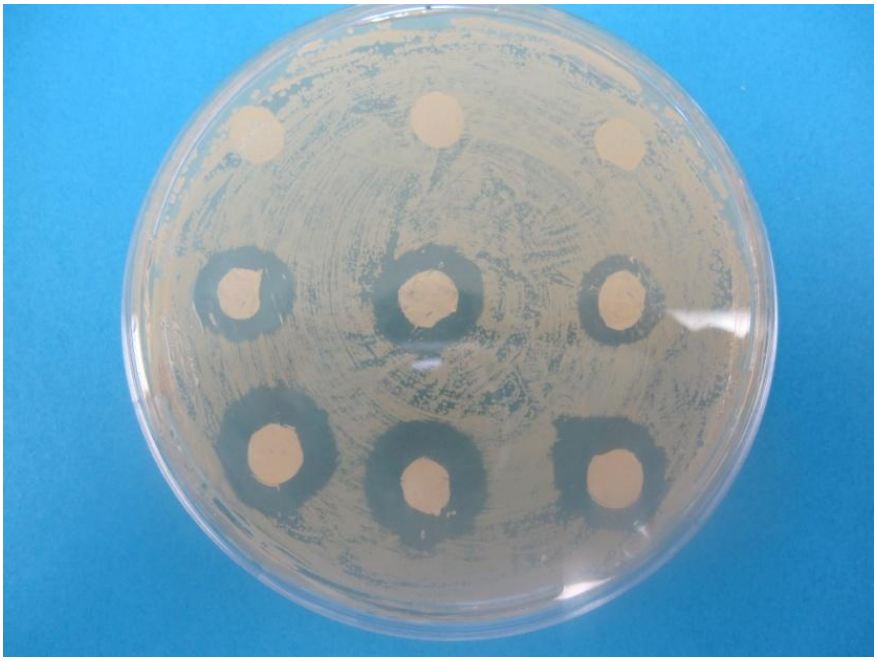

Figure 32: Biological results after 1 day. Top row are samples with 20% HA and 0% Gentamicin, middle row are samples with 20% HA and 5% Gentamicin, and bottom row are samples with 20% HA and 10% Gentamicin.

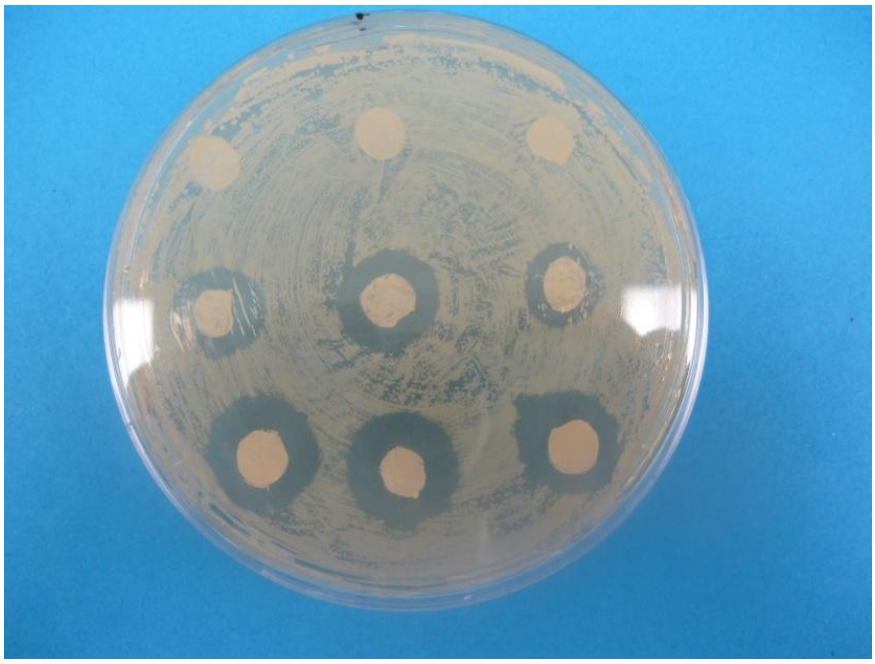

Figure 33: Biological results after 2 days. Top row are samples with 20% HA and 0% Gentamicin, middle row are samples with 20% HA and 5% Gentamicin, and bottom row are samples with 20% HA and 10% Gentamicin.

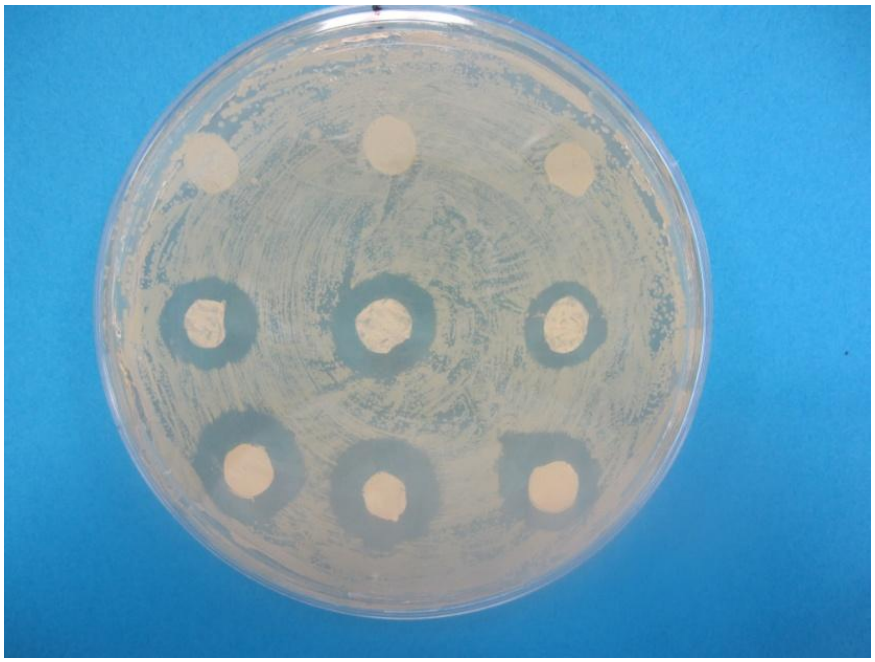

Figure 34: Biological results after 5 days. Top row are samples with 20% HA and 0% Gentamicin, middle row are samples with 20% HA and 5% Gentamicin, and bottom row are samples with 20% HA and 10% Gentamicin.

Figure 35 though Figure 37 show samples of 0% HA, 5% gentamicin; 5% HA, 5% gentamicin; 10% HA, 5% gentamicin taken one, three and four days after initial culture, respectively. All of these samples have a zone of inhibition which is good since all of the samples contain gentamicin. Since all of the samples have a gentamicin concentration of 5%, the size of the zone of inhibition for each sample should be similar. As can be seen in the figures, there is a difference in size of zone of inhibition for each set of samples. The reasons for these differences will be discussed below. Like with the previous set of samples, there is no visual difference between the sizes of the zone of inhibition throughout the days after initial culture.

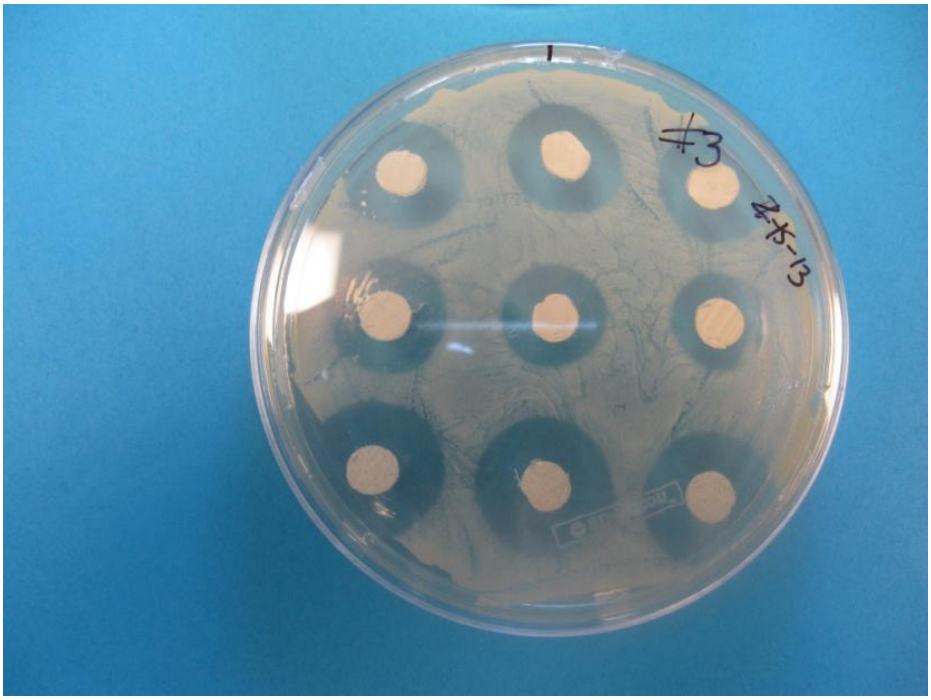

Figure 35: Biological results after 1 day. Top row are samples with 0% HA and 5% Gentamicin, middle row are samples with 5% HA and 5% Gentamicin, and bottom row are samples with 10% HA and 5% Gentamicin.

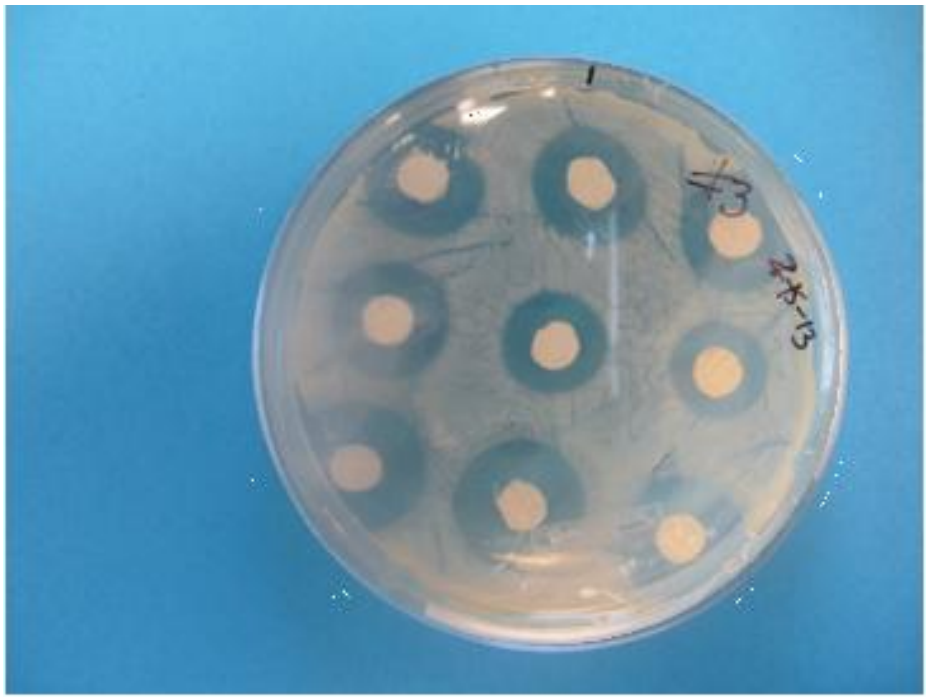

Figure 36: Biological results after 3 days. Top row are samples with 0% HA and 5% Gentamicin, middle row are samples with 5% HA and 5% Gentamicin, and bottom row are samples with 10% HA and 5% Gentamicin.

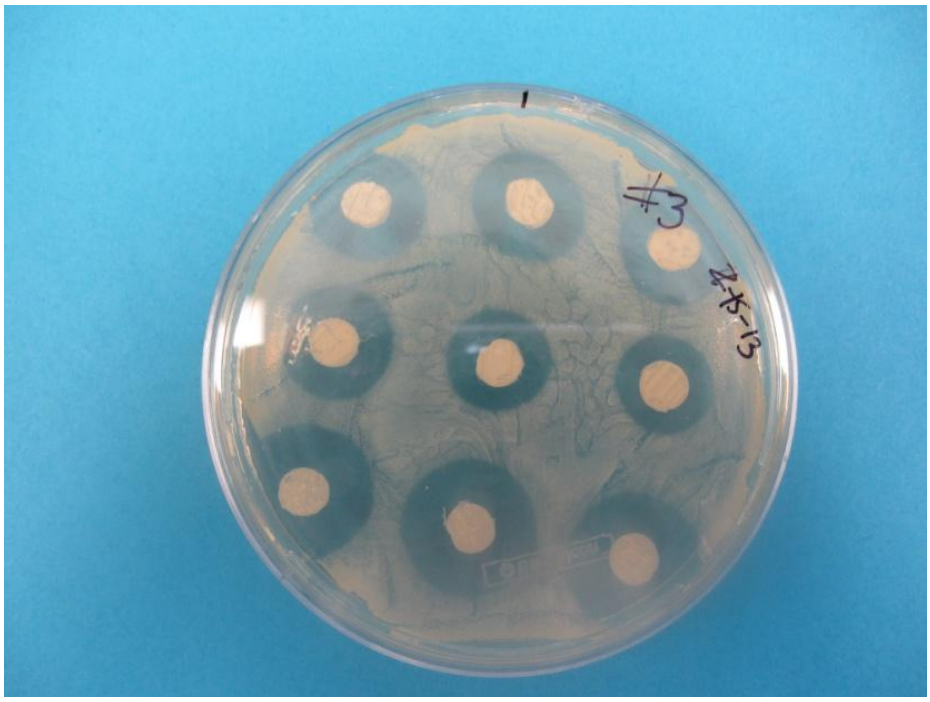

Figure 37: Biological results after 4 days. Top row are samples with 0% HA and 5% Gentamicin, middle row are samples with 5% HA and 5% Gentamicin, and bottom row are samples with 10% HA and 5% Gentamicin.

Finally, Figure 38 through Figure 40 show samples of 0% HA, 10% gentamicin; 5% HA, 10% gentamicin; and 10% HA, 10% gentamicin after one, three, and four days. Again with all of the previous gentamicin samples, there is a zone of inhibition around the sample showing that the gentamicin is active. Like with the 5% gentamicin samples, there is a size difference in the zone of inhibition between different sets of samples whereas the size should be similar. Also, like the rest of the samples, there was no difference in the size of the zone of inhibition between days images were taken.

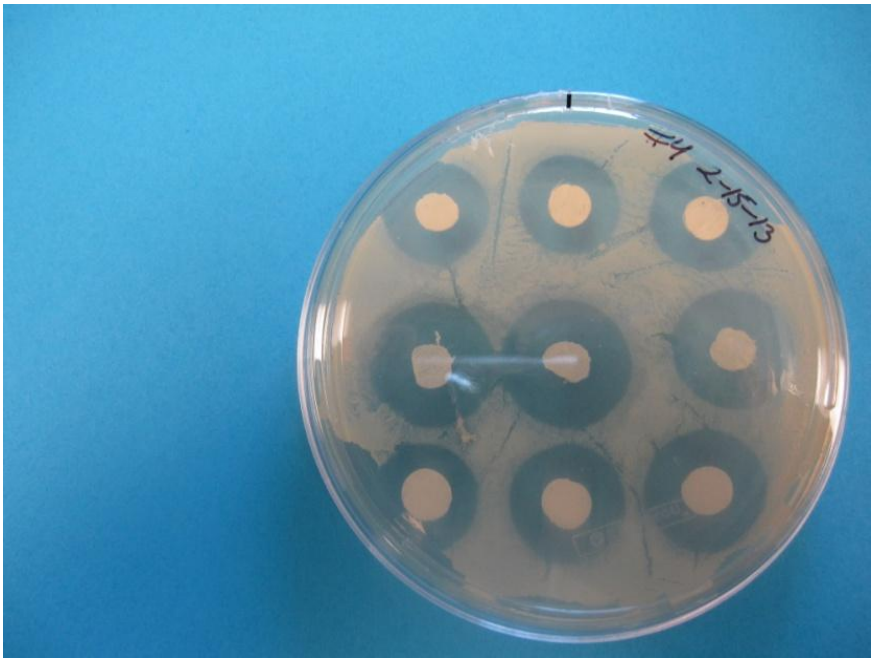

Figure 38: Biological results after 1 day. Top row are samples with 0% HA and 10% Gentamicin, middle row are samples with 5% HA and 10% Gentamicin, and bottom row are samples with 10% HA and 10% Gentamicin.

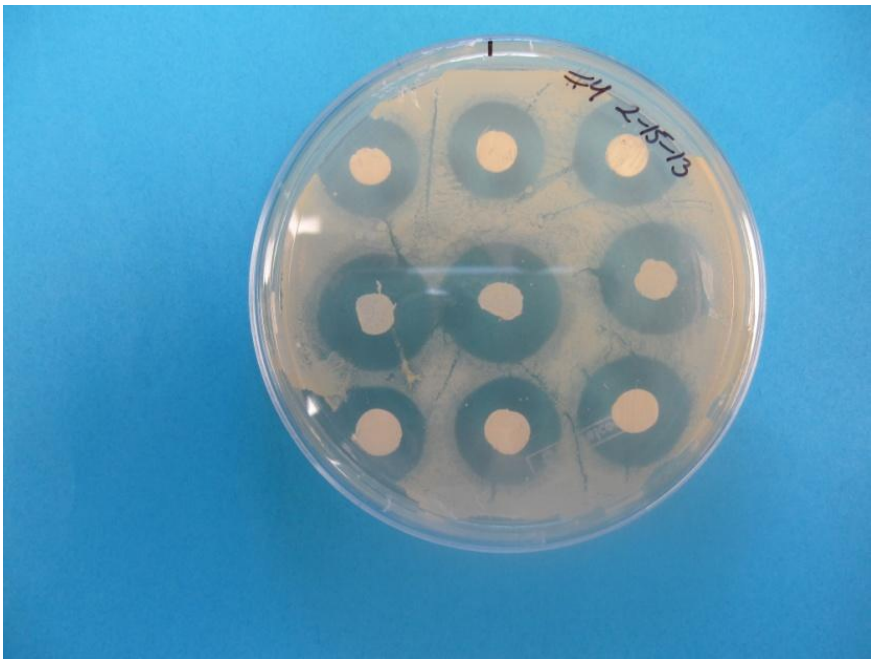

Figure 39: Biological results after 3 days. Top row are samples with 0% HA and 10% Gentamicin, middle row are samples with 5% HA and 10% Gentamicin, and bottom row are samples with 10% HA and 10% Gentamicin.

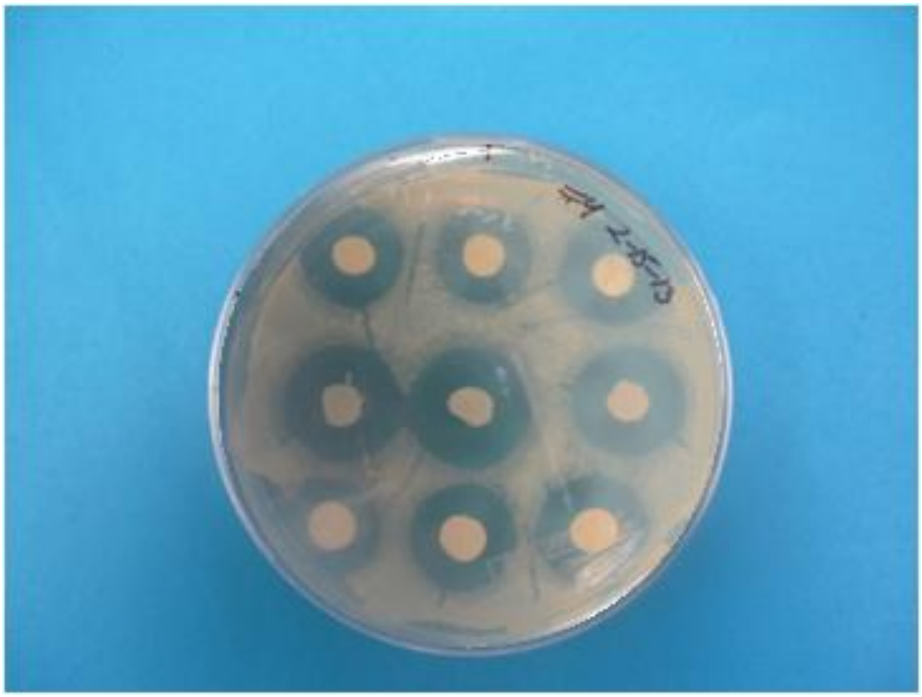

Figure 40: Biological results after 4 days. Top row are samples with 0% HA and 10% Gentamicin, middle row are samples with 5% HA and 10% Gentamicin, and bottom row are samples with 10% HA and 10% Gentamicin.

Figure 41 and Figure 42 show the average area of the zone of inhibition for all of the gentamicin samples. This result is comparable to that demonstrated by Threepopnatkul et al., although they demonstrated the behavior with the gram-positive bacteria Staphylococcus aureus. [39] This is significant, as gram-positive bacteria are more susceptible to antibacterial agents such as gentamicin. Furthermore, a study by Torres-Giner et al performed bacterial susceptibility tests with PLA electrospun fibers with gentamicin. The bacteria used for the testing were Staphylococcus epidermis, Pseudomonas aeruginosa, and E. coli. Their results showed that S. epidermis was the most susceptible to the PLA and gentamicin fibers while P. aeruginosa was the most resistant. E. coli was shown to have moderate susceptibility between the other two with an extreme drop off in bacterial colonies at a much lower gentamicin concentration than P. aeruginosa. Since S. epidermis is also a gram-positive bacterium while P. aeruginosa is gram-negative, these results follow known performance trends. [40] The results outlined in this thesis also correlate well to these trends.

Despite fluctuations between gentamicin samples at different HA concentrations, there was no significant difference in area for samples of the same chemical content (HA and gentamicin percentage) using Student t-test with a 95% confidence. Some possible causes for the fluctuations in zone of inhibition area include:

- Agar solution in petri dishes that weren't level, which could cause more bacteria to be accumulated in low spots.
- Uneven spreading of bacteria, which would obviously cause uneven colony growth.

The growth of bacterial colonies located near antibacterial samples which are too close to each other or the edge of the petri dish could grow unevenly; due to growth inhibition in one direction, colonies may grow disproportionately in another – skewing the results.

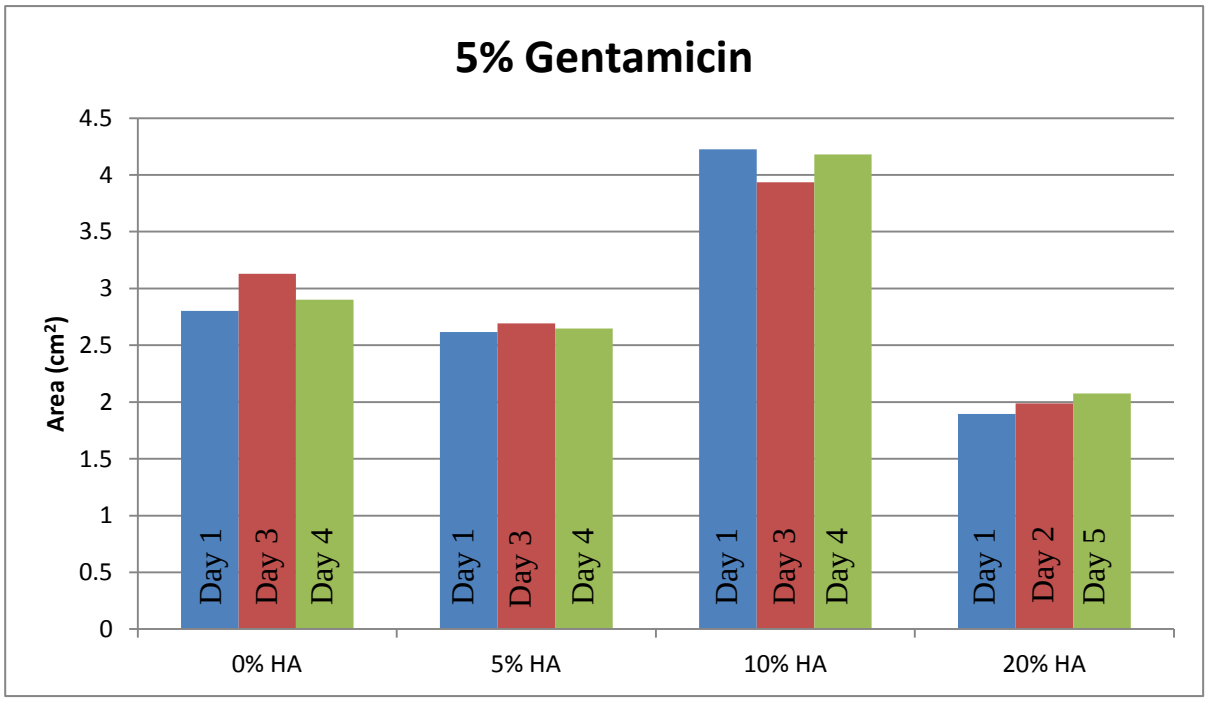

Figure 41: Area of zone of inhibiton of 5% gentamicin samples.

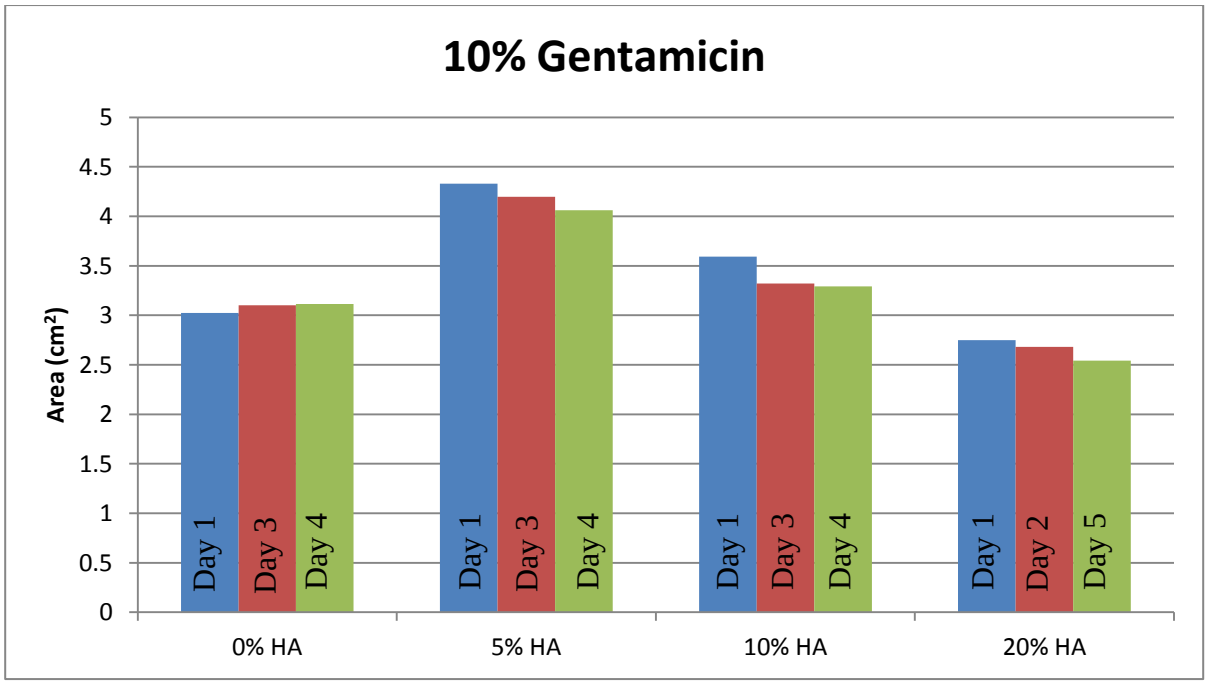

Figure 42: Area of zone of inhibition of 10% gentamicin samples.

CHAPTER 5

CONCLUSION AND FUTURE WORK

5.1 Conclusions

PCL nanofibers were successfully fabricated using electrospinning; the nanofibers incorporate both HA and gentamicin. The following procedure was used to fabricate and test the samples:

1. PCL, DMF, DCM, HA, and gentamicin were mixed together to create a polymer solution for electrospinning.
2. The polymer solution was electrospun.
3. Nano-sized PCL fibers were dried and collected.
4. SEM micrographs and anti-bacterial susceptibility tests were performed.

SEM micrographs showed that the fibers are truly on a nano-scale and have the HA particles embedded within them. Additionally, the SEM images provide visual confirmation that the fibers form interconnected pores – which will allow for healthy development of new tissues, without necrosis. Although there was initially a concern that the use of Dimethylformamide and Dichloromethane solvents and the electrospinning process might damage the gentamicin, biological testing showed that the gentamicin successfully remained active and was effective as an antibacterial agent against E. coli. The inclusion of natural HA in the composite nanofibers will encourage the growth of osteoblast cells, when used in a 3-D bone tissue scaffold. Although at the time of this study natural HA has not been demonstrated to be superior or inferior in performance as compared to synthesized HA, this method successfully demonstrated that HA derived from natural bone can be used in an electrospinning process to develop a PCL-HA nanofiber composite. This allows for an alternative source of HA, as compared to what has been

demonstrated in other studies.

5.2 Future Work

- Adjusting the solvent mixture or adding a salt to the polymer mixture in order to eliminate beads from the fibers.
- Another biological study with a less diluted E. coli solution should be performed. The samples presented in this study demonstrated no difference in zone of inhibition for up to four or five days after initial culture. A less diluted solution should show a zone of inhibition trend that grows larger for a couple of days, and then becomes smaller again as all of the gentamicin is consumed.
- Cell toxicity testing should be performed to ensure that there is nothing present on or in the nanofibers that would cause harm to cells or the host. Even though the nanofibers were dried for over 48 hours, the solvents used are not biocompatible and remnants could be present. As such, cell toxicity testing is necessary to ensure the full biocompatibility of the nanofibers.
- Culturing of osteoblasts onto the nanofibers should be perfomed in order to show the nanofiber's viability as a scaffold material.
- The final step to demonstrating PCL-HA nanofibers as a viable bone tissue scaffold is to shape them into a 3-D structure that can serve as an effective bone tissue scaffold. This scaffold should then undergo a battery of tests, including in vivo, to ensure suitability for application as a bone defect repair technique.
- Alternative manufacturing methods can be attempted, using the same PCL-HA composite. Potential methods are discussed in Section 2.3.5; these include salt and polymer leaching techniques, among others.

REFERENCES

REFERENCES

[1] H. Cao, L.-b. Chen, Y.-s. Liu, H. Xiu and H. Wang, "Poly-D, L-Lactide and Levofloxacin-Blended Beads: A Sustained Local Releasing System to Treat Osteomyelitis," *Journal of Applied Polymer Science,* vol. 124, pp. 3678-3684, 2012.

[2] A. El-Ghannam, K. Ahmed and M. Omran, "Nanoporous Delivery System to Treat Osteomyelitis and Regenerate Bone: Gentamicin Release Kinetics and Bactericidal Effect," *Journal of Biomedical Materials Research - Part B Applied Biomaterials,* vol. 73, no. 2, pp. 277-284, 2004.

[3] H. Tan, Z. Peng, Q. Li, X. Xu, S. Guo and T. Tang, "The use of quaternised chitosan-loaded PMMA to inhibit biofilm formation and downregulate the virulence-associated gene expression of antibiotic-resistant staphylococcus," *Biomaterials,* vol. 33, pp. 365-377, 2012.

[4] H. Yu, P. J. VandeVord, L. Mao, H. W. Matthew, P. H. Wooley and S.-Y. Yang, "Improved tissue-engineered bone regeneration by endothelial cell mediated vascularization," *Biomaterials,* pp. 508-517, 2009.

[5] A. Jabbarnia, V. R. Patlolla, H. E. Misak and R. Asmatulu, "Electrospun Fibers Incorporated with Hydroxyapatite Nanoparticles and Graphene Nanoflakes for Bone Scaffolding," in *ASME 2012 International Mechanical Engineering Congress & Exposition*, Houston, TX, 2012.

[6] W. F. Zambuzzi, C. V. Ferreira and J. M. Granjeiro, "Biological behavior of pre-osteoblasts on natural hydroxyapatite: A study of signaling molecules from attachment to differentiation," *Journal of Biomedical Materials Research A,* vol. 97A, no. 2, pp. 193-200, 2011.

[7] J. R. Jones, "Scaffolds for tissue engineering," in *Biomaterials*, 2005, pp. 201-214.

[8] L. Lao, Y. Wang, Y. Zhu, Y. Zhang and C. Gao, "Poly(lactide-co-glycolide)/hydroxyapatite nanofibrous scaffolds fabricated by electrospinning for bone tissue engineering," *Journal of Materials Science: Materials in Medicine,* vol. 22, pp. 1873-1884, 2011.

[9] F. A. Sheikh, N. A. M. Barakat, M. A. Kanjwal, R. Nirmala, J. H. Lee, H. Kim and H. Y. Kim, "Electrospun titanium dioxide nanofibers containing hydroxyapatite and silver nanoparticles as future implant materials," *Journal of Materials Science: Materials in Medicine,* vol. 21, pp. 2551-2559, 2010.

[10] J. W. Hench, "Cells and tissues," in *Biomaterials*, 2005, pp. 59-70.

[11] L. L. Hench, "The skeletal system," in *Biomaterials*, 2005, pp. 79-89.

[12] L. L. Hench, "Repair of skeletal tissues," in *Biomaterials,* 2005, pp. 119-128.

[13] Central Washington University, "Anatomical Kinesiology: Types of Fractures, healing, and clinical advances in bone repair.," [Online]. Available: http://www.cwu.edu/~acquisto/fractures.htm. [Accessed 8 May 2013].

[14] J. W. Hench, "Inflammation and wound healing," in *Biomaterials,* 2005, pp. 71-76.

[15] J. Selvakumaran and G. Jell, "A guide to basic cell culture and applications in biomaterials and tissue engineering," in *Biomaterials,* 2005, pp. 215-226.

[16] G. Jell and J. Selvakumaram, "Immunochemical techniques in tissue engineering and biomaterial science," in *Biomaterials,* 2005, pp. 227-240.

[17] H. Yu, H. W. Matthew, P. H. Wooley and S.-Y. Yang, "Effect of Porosity and Pore Size on Microstructures and Mechanical Properties of Poly-ε-Caprolactone-Hydroxyapatite Composites," *Journal of Biomedical Materials Research Part B: Applied Biomaterials,* pp. 541-547, 2008.

[18] L. L. Hench and J. R. Jones, "Clinical applications of tissue engineering," in *Biomaterials,* 2005, pp. 241-248.

[19] A. Salerno, D. Guarnieri, M. Iannone, S. Zeppetelli and P. A. Netti, "Effect of Micro- and Macroporosity of Bone Tissue Three-Dimensional-Poly(ε-Caprolactone) Scaffold on Human Mesenchymal Stem Cells Invasion, Proliferation, and Differentiation In Vitro," *Tissue Engineering: Part A,* vol. 16, no. 8, pp. 2661-2673, 2010.

[20] S. M. Mantila Roosa, J. M. Kemppainen, E. N. Moffitt, P. H. Krebsbach and S. J. Hollister, "The pore size of polycaprolactone scaffolds has limited influence on bone regeneration in an in vivo model," *Journal of Biomedical Materials Research Part A,* pp. 359-368, 2009.

[21] C. M. Murphy, M. G. Haugh and F. J. O'Brien, "The effect of mean pore size on cell attachment, proliferation and migration in collagen-glycosaminoglycan scaffolds for bone tissue engineering," *Biomaterials,* pp. 461-466, 2010.

[22] S.-W. Choi, Y. Zhang and Y. Xia, "Three-Dimensional Scaffolds for Tissue Engineering: The Importance of Uniformity in Pore Size and Structure," *Langmuir,* pp. 19001-19006, 2010.

[23] T. Tanaka, S. Eguchi, H. Saitoh, M. Taniguchi and D. R. Lloyd, "Microporous foams of polymer blends of poly(L-lactic acid) and poly(ε-caprolactone)," *Desalination,* pp. 175-183, 2008.

Q. Zhang, W. Zhang, J. Augustin, D. Yao, D. M. Wootton, F. A. Kleinbart, N. A. Johanson,

[24] K. A. Wasko, P. I. Lelkes and J. G. Zhou, "Bio-Testing of Poly-L-Lactic Acid/Hydroxyapatite Porous Bone Scaffolds," in *ASME 2011 International Mechanical Engineering Congress & Exposition*, Denver, CO, 2011.

[25] T.-M. Wu and E.-C. Chen, "Isothermal and Nonisothermal Crystallization Kinetics of Poly(ε-caprolactone)/Multi-Walled Carbon Nanotube Composites," *Polymer Engineering and Science*, pp. 1309-1317, 2006.

[26] B. Gupta, S. Patra and A. R. Ray, "Preparation of Porous Polycaprolactone Tubular Matrix by Salt Leaching Process," *Journal of Applied Polymer Science,* vol. 126, pp. 1505-1510, 2012.

[27] I. Polysciences, "Polycaprolactone, Powdered," [Online]. Available: http://www.polysciences.com/Catalog/Department/Product/98/categoryid--286/productid--2923/. [Accessed 7 April 2013].

[28] H. Altpeter, M. J. Bevis, D. W. Grijpma and J. Feijen, "Non-conventional injection molding of poly(lactide) and poly(ε-caprolactone) intended for orthopedic applications," *Journal of Materials Science: Materials in Medicine*, pp. 175-184, 2004.

[29] R. G. Hill, "Biomedical polymers," in *Biomaterials*, 2005, pp. 97-106.

[30] F. Simonovsky, "Biomaterials Tutorial," [Online]. Available: http://www.uweb.engr.washington.edu/research/tutorials/plagla.html. [Accessed 18 April 2013].

[31] T. P. James and B. A. Andrade, "Is Synthetic Composite Bone a Substitute for Natural Bone in Screw Bending Tests," in *Proceedings of the ASME 2011 International Mechanical Engineering Congress & Exposition*, Denver, 2011.

[32] L. Calandrelli, B. Immirzi, M. Malinconico, S. Luessenheide, I. Passaro, R. Di Pasquale and A. Oliva, "Natural and Synthetic Hydroxyapatite Filled PCL: Mechanical Properties and Biocompatibility Analysis," *Journal of Bioactive and Compatible Polymers,* vol. 19, pp. 301-313, 2004.

[33] D. Kopeliovich, "Injection Molding of Polymers," [Online]. Available: http://www.substech.com/dokuwiki/doku.php?id=injection_molding_of_polymers. [Accessed 9 April 2013].

[34] M. Song, M. S. Park, J. K. Kim, I. B. Cho, K. H. Kim, H. J. Sung and S. Ahn, "Water-soluble binder with high flexural modulus for powder injection molding," *Journal of Materials Science,* vol. 40, pp. 1105-1109, 2005.

P. Lu and B. Ding, "Applications of Electrospun Fibers," *Recent Patents on*

[35] *Nanotechnology,* vol. 2, no. 3, pp. 169-182, 2008.

[36] J. Gatford, "Electrospinning Diagram," 8 September 2008. [Online]. Available: http://en.wikipedia.org/wiki/File:Electrospinning_Diagram.jpg. [Accessed 8 April 2013].

[37] N. E. Zander, J. A. Orlicki, A. M. Rawlett and T. P. Beebe Jr., "Electrospun polycaprolactone scaffolds with tailored porosity using two approaches for enchanced cellular infiltration," *Journal of Materials Science: Materials in Medicine,* 2012.

[38] Y. Liu, J.-H. He, J.-y. Yu and H.-m. Zeng, "Controlling numbers and sizes of beads in electrospun nanofibers," *Polymer International,* vol. 57, pp. 632-636, 2008.

[39] P. Threepopnatkul, K. Vichitchote, S. Saewong, T. Tangsupa-Anan, C. Kulsetthanchalee and S. Suttiruengwong, "Mechanical and Antibacterial Properties of Electrospun PLA/PEG Mats," *Journal of Metals, Materials and Minerals,* pp. 185-187, 2010.

[40] S. Torres-Giner, A. Martinez-Abad, J. V. Gimeno-Alcañiz, M. J. Ocio and J. M. Lagaron, "Controlled Delivery of Gentamicin Antiobiotic from Bioactive Electrospun Polylactide-Based Ultrathin Fibers," *Advanced Biomaterials,* vol. 14, no. 4, pp. B112-B122, 2012.

[41] L. D. K. Buttery and A. E. Bishop, "Introduction to tissue engineering," in *Biomaterials,* 2005, pp. 193-200.

[42] O. Emohare and N. Rushton, "Immobilized MWCNT support osteogenic cell culture," *Journal of Materials Science: Materials in Medicine,* 2013.

[43] D. Liu, L. Wang, Z. Wang and A. Cuschieri, "Different cellular response mechanisms contribute to the length-dependent cytotoxicity of multi-walled carbon nanotubes," *Nanoscale Research Letters,* vol. 7, 2012.